Impact of Cross-Phase Modulation on Fiber-Optic Communication System in Presence of First- and Second Order Group Velocity Dispersion

by

Muhammad Abul Khayer Azad

MASTER OF SCIENCE IN INFORMATION AND COMMUNICATION TECHNOLOGY

Institute of Information and Communication Technology

Bangladesh University of Engineering and Technology

March, 2010

This thesis titled "**Impact of Cross-Phase Modulation on Fiber-Optic Communication System in Presence of First- and Second Order Group Velocity Dispersion"** Submitted by **Muhammad Abul Khayer Azad, Roll No: M10053103P, Session: October 2005** has been accepted as satisfactory in partial fulfillment of the requirements for the degree of Master of Science in Information and Communication Technology on March 9, 2010.

BOARD OF EXAMINERS

	_____	Chairman
1.	Dr. Md. Saiful Islam Associate Professor Institute of Information and Communication Technology Bangladesh University of Engineering and Technology Dhaka-1000, Bangladesh	
	_____	Member
2.	Dr. S. M. Lutful Kabir Professor and Director Institute of Information and Communication Technology Bangladesh University of Engineering and Technology Dhaka-1000, Bangladesh	(Ex-Officio)
	_____	Member
3.	Md. Rubaiyat Hossain Mondal Assistant Professor Institute of Information and Communication Technology Bangladesh University of Engineering and Technology Dhaka-1000, Bangladesh	
	_____	Member
4.	Md. Mujibur Rahman Managing Director Teletalk Bangladesh Limited Dhaka-1213, Bangladesh.	(External)

DECLARATION

It is hereby declared that this thesis or any part of it has not been submitted elsewhere for the award of any degree or diploma.

Muhammad Abul Khayer Azad

DEDICATED TO MY PARENTS

CONTENTS

List of Figures

List of Tables

List of Abbreviations

A = Pulse amplitude

ASE = Amplifier Spontaneous Emission Noise

ASK = Amplitude Shift Keying

APD = Avalanche photodiode

BER = Bit Error Rate

CW = Continuous Wave

DCF = Dispersion Compensating Fiber

DWDM = Dense Wavelength Division Multiplexing

EDFA = Erbium-Doped Fiber Amplifier

F = Frequency [GHz]

FBG = Fiber Bragg Grating

FWM = Four-Wave Mixing

GVD = Group Velocity Dispersion

L = Fiber length [km]

n = Refractive index

n_2 = Refractive index of the cladding

NRZ = Non-Return-to-Zero bit format

P = Power average in single channel [dBm] or [*mW*]

PMD = Polarisation Mode Dispersion

Q = Q-factor

R = Resistance [Ω]

RZ = Return-to-Zero bit format

SBS = Stimulated Brillouin Scattering

SNR = Signal-to-Noise Ratio

SMF = Single-Mode Fibre

SPM = Self-Phase Modulation

SRS = Stimulated Raman Scattering

WDM = Wavelength Division Multiplexing

XPM = Cross-Phase Modulation

Acknowledgements

I am highly pleased to express my sincere and profound gratitude to my supervisor Dr. Md. Saiful Islam, for providing me the opportunity to conduct graduate research in optical communications. I wish my hearty thanks to him for his continuous guidance, suggestions and wholehearted help throughout the course of the work. I gratefully acknowledge the advice and encouragement from all of my honorable teachers at IICT, BUET.

I would like to express my special thanks to the Management of Investment Corporation of Bangladesh (ICB) for providing me permission and support to continue my study and research works. I would also like to thank my colleagues for their support and continuous encouragement. I would also like to express my heartfelt gratitude to all the unseen contributions.

I like to express my deepest gratitude to my wife Sabia Akter, my beloved daughter Khadiza binte Khayer and other family members for their invaluable encouragement and patience.

Finally, I am grateful to almighty Allah for enabling me to complete the thesis.

Abstract

With the increasing demands on the capacity of WDM systems, cross-phase modulation (XPM) has become the most significant nonlinear effect and limits the system performance. On the other hand, group velocity dispersion (GVD) is one of the linear effects in the optical fiber that also restricts bit rates. As a result, the combined effects of GVD and XPM may cause further deterioration of transmission performance in a WDM system. In this research work, an analytical model for a WDM system is developed incorporating the combined effects of XPM, first- and second order GVD. The crosstalk expression for the affected channel is derived in terms of system parameters for standard single mode fiber (SSMF), dispersion shifted fiber (DSF) and large effective area fiber (LEAF).

The spectral characteristics are strongly dependent on the channel spacing and GVD of the fiber *i.e*. the crosstalk effect is more at narrow channel spacing and lower GVD. It is found that at 10 GHz modulation frequency and 0.8nm channel spacing for 100 km distance DSF suffers XPM crosstalk penalty 23 dB and 16 dB more than SSMF for first order GVD and second order GVD respectively. The crosstalk effect due second order GVD is found insignificant in presence of first order GVD in single span system, but at high bit rate and long haul first order GVD compensated system, the effect of second order GVD become significant and play a critical role in limiting the system performance. Simulation results show that system suffers maximum penalty due to XPM effect at zero dispersion coefficient and XPM interference is linearly dependent on optical power of the injected signals in a very large range of system parameters. It is also found that system bit error rate and eye opening penalty is high at higher value of GVD. Among the 3-types of fiber, SSMF contributes least amount of XPM crosstalk for the same amount of pumps and probe power. Thus the findings of this thesis can predict accurate amount of crosstalk due to XPM and may be useful to design a WDM optical communication system.

CHAPTER 1

Introduction

1.1 Communication system

Communication means the exchange of information which may be voice, video or data. So, a communication system transmits information from one place to another place. Communication systems exchange signals between two or more entities in a form suitable to process and manipulate most economically. The basic principle of a communication system is to bridge two entities at different locations.

Twenty first century is the era of information technology (IT). There is no doubt that IT has achieved an exponential growth through the modern telecommunication systems. Particularly, optical fiber communication plays a vital role in the development of high quality and high-speed telecommunication systems. Today, optical fibers are not only used in telecommunication links but also used in the Internet and local area networks (LAN) to achieve high signaling rates. In the recent years, the advent of erbium-doped fiber amplifier (EDFA) is one of the most notable breakthroughs in the fiber optical communication technology [1].

Before the emergence of EDFAs, the standard method of compensating fiber loss was to place electronic regenerators periodically along the transmission link. A regenerator consists of photo-detectors, electronic processing and amplification block and a transmitter. Functionally, it performs optical to electronic conversion, electronic processing and electrical to optical, conversion and retransmission of the regenerated signal. The advantages of regenerative systems are that transmission impairments such as noise, dispersion and nonlinearities do not accumulate, which makes it easy to design transmission links. However electronic blocks in regenerator prevent exploitation of the huge bandwidth of the fiber. Electronics components are normally designed for the specific bit rate and modulation format, it is necessary to replace all the regenerative repeaters along the link when the system capacity must be increased. On the other hand, optical amplifiers like EDFAs simply amplify the optical signal by several orders of magnitude without being limited by electronic speed. In addition amplification is bit rate and modulation format independent, which implies that optically amplified links,

can be upgraded by replacing terminal equipment alone. The optically amplified transmission lines can be considered as a transmission pipe, which is transparent to data rate and signal modulation format.

Optical transmission is a preferred medium for long distance, high bandwidth communication system running at speeds in the range of gigabit per second or higher. The process towards ever increasing speeds encounters an obstacle in the form of the group velocity dispersion (GVD) in the optical fiber that restricts bit rates [2]-[3]. On the other hand, the progress towards longer lengths of transmission has led to increasing input power and at higher power, nonlinear effect is introduced in the optical fiber that in turn also limits the transmission distance of optical signal [4]-[5]. In late 1990s wavelength division multiplexing (WDM) systems have been widely deployed as a solution for higher bit rate transmission. With the increasing demands on the capacity of WDM systems, crosstalk due to nonlinearity become important and cross-phase modulation (XPM) is one of the most significant nonlinear effects that impact the system performance [6]-[7]. As a result, the combined effects of GVD and XPM may cause further deterioration of transmission performance in a WDM system. Thus, it is essential to study the impact of XPM and GVD to predict the performance limitation or system outage accurately due to these effects in the WDM transmission system.

1.2 Evolution of optical communication

Even though an optical communication system had been conceived in the late 18^{th} century by a French Engineer Claude Chappe who constructed an optical telegraph, electrical communication systems remained the dominant means of communication. In 1966, Kao and Hockham proposed the use of optical fiber as a guiding medium for the optical signal [8]. Four years later, a major breakthrough occurred when the fiber loss was reduced to about 20 dB/km from previous values of more than 1000 dB/km by applying improved fiber manufacture and design techniques. Since that time, optical communication technology has developed rapidly to achieve larger transmission capacity and longer transmission distance. The capacity of transmission has been increased about 100 fold in every 10 years.

There were several major technological breakthroughs during the past two decades to achieve such a rapid development. In 1980, the bit rate used was 45 Mb/s

with repeater spacing of 10 km. The multimode fiber was used as the transmission medium and GaAs LED as the source of the system. In 1987 the bit rate was increased to 1.7 Gbps with repeater spacing of 50 km. By 1990 the bit rate was increased to 2.5 Gbps with repeater spacing further increased to 60-70 km. Dispersion shifted fibers are used to minimize the bit error rate and to increase the repeater spacing and the bit rate.

In 1996, the bit rate of the optical transmission system was increased to 5 Gbps. The development of optical amplifiers brought another important break through in optical communication system. Optical amplifiers reduced the associated delay and power requirement of the electronic amplifiers. WDM was also introduced at this time to increase the available bandwidth capacity in terms of the channels. By 2002, the bit rate of the optical system was increased to 10 Gbps with repeater spacing of 70-80 km. The introduction of the dense-wavelength division multiplexing (DWDM) system increased the channel capacity and the bit rate got increased to 40 Gbps.

The first generation of optical communication was designed with multi-mode fibers and direct band gap GaAs Light emitting diodes (LEDs) which used to operate at the 0.8 μm – 0.9 μm wavelength range. Compared to the typical repeater spacing of coaxial system (~1 km), the longer repeater spacing (~10 km) was a major motivation. Large model dispersion of multi-mode fibers and high fiber loss at 0.8 μm (>5dB/km) limited both the transmission distance and bit rate. In the second generation, multi-mode fibers were replaced by single- mode fibers, and the center wavelength of light sources was shifted to 1.3μm, where optical fibers have minimum dispersion and lower loss of about 0.5 dB/km.

However, there was still a strong demand to increase repeater spacing further, which could be achieved by operating at 1.55 μm where optical fibers have an intrinsic minimum loss around 0.2 dB/km. Larger dispersion in the 1.55 μm window delayed moving to a new generation until dispersion shifted fiber became available. Dispersion shifted fibers reduced the large amount of dispersion in the 1.55 μm window by modifying the index profile of the fibers while keeping the benefit of low loss at the 1.55 μm window. However, growing communication traffic and demand for larger bandwidth per user revealed a significant drawback of electronic regeneration systems. Because all the regenerators are designed to operate at specific data rate and modulation format, all of them needed to be replaced to convert to a higher data rate.

The difficulty of upgradeability has finally been removed by optical amplifiers, which led to a completely new generation of optical communication. An important advance was that an EDFA at 1.55 μm was found to be ideally suited as an amplifying medium for modern fiber optic communication systems. Invention of the EDFA had a profound impact especially on the design of long haul under sea systems. Trans-oceanic systems installed like TAT (Transatlantic Telephone)-12/13 [9] and TPC (Transpacific Crossings)-5 [10] were designed with EDFA's and the transmission distance reaches over 8000 km without electronic repeaters between terminals. The broad gain spectrum (3 ~ 4 THz) of an EDFA also makes it practical to implement WDM systems.

It is highly likely that DWDM systems will bring another big leap of transmission capacity of optical communication systems. Some research groups have already demonstrated that it is possible to transmit almost a Tbps bit rate over thousands of kilometers. There are some important experimental results of DWDM systems [11]. In 1999, a channel system was simulated experimentally with bit rate 20 Gbps. The system could cover 10,000 km with amplifier spacing of 50 km. The signal format used here was of soliton type. Later the number of channels was increased to 32 with 45 km amplifier spacing and the distance covered was 9,300 km. In this system NRZ and soliton type signal format were used.

In 1998, the number of the channels was increased to 64 at the cost of reduced transmission distance of 500 km with 100 km amplifier spacing. However by 1999 the distance could be extended to 7,200 km with 64 channel system and 10 Gbps bit rate at the cost of reduced amplifier spacing of 50 km. In 2004, the bit rate was increased to 40 Gbps at the cost of reduced number of channels of 34 which could cover a distance of 6,380 km. These results indeed show that remarkable achievements have been made in recent years, and let us forecast that optical communication systems in the next generation will have a transmission capacity of a few hundreds of Gbps [12].

1.3 Review of previous works

Over the years, lot of research works has been carried out to study the harmful impact of fiber nonlinearity on optical transmission system. Among the different types

of fiber nonlinearities, the XPM effect is found to be more detrimental in limiting system performance. In the following section, we are describing some of the research works those are carried out to evaluate the impact of XPM in WDM optical transmission system.

Hui *et al.* (1998) evaluated spectral characteristics of XPM in multi-span WDM systems both experimentally and theoretically [14]. They found that the crosstalk level is dependent on optical channel spacing and fiber dispersion. Interference between XPM crosstalk generated in different fiber spans creates strong ripples in the frequency response. A simple analytical expression was obtained to describe the XPM-induced crosstalk.

Majumder *et al.* (1998) analytically evaluated the impact of GVD on the BER performance of a WDM optical network [15]. They have shown that the performance of the system highly degrades in presence of fiber dispersion and presence of dispersion imposes several restrictions on the number of nodes and the node spacing.

Kenneth *et al.* (1999) also investigated the spectral characteristics of XPM in multispan IM-DD optical systems, both experimentally and theoretically [16]. The have shown that Interference between XPM-induced crosstalk components created in different amplified fiber spans has a strong impact on the overall frequency response of XPM crosstalk in the system. Reasonably good agreement between theory and experiment has been obtained. In uncompensated optical systems, a decrease in fiber dispersion will increase XPM-induced phase modulation efficiency, while an increase in fiber dispersion will increase phase-to-intensity noise conversion efficiency. Dispersion compensation was shown to be an effective way to reduce XPM-induced crosstalk in IM-DD systems. Different schemes of dispersion compensation in multi-span optical fiber systems were evaluated and per span dispersion compensation was found to be the most effective way to minimize the effect of XPM crosstalk. The crosstalk level between high and low bit rate channels was found to be similar to that between two low bit rate channels. This is due to the effect of the base band filter in the optical receivers.

Thiele *et al.* (1999) investigated the effect of pre- and post compensation in high capacity WDM systems with large inter amplifier spacing [17]. They measured spectral

broadening by using a gated, scanning interferometer. It was shown that in the case of post compensation, the eye closure was more rapid in the post compensation case. With 4 channel transmission little change in the SPM penalty was observed. This was attributed to the XPM induced timing jitter and to crosstalk between channels at the receiver due to spectral broadening. For the case of pre compensation in a 4 channel system, large broadening was observed due to high peak power of the compressed pulses at the start of each span increasing the effects of SPM and XPM. The limitation imposed by SPM in post compensated systems can be overcome by pre compensated systems.

Killey *et al.* (2000) demonstrated the accuracy of predicting penalties from the distortion of a CW Probe channel using pump probe configuration both experimentally and theoretically [18].

Hoon (2003) investigated, theoretically and experimentally the SPM and XPM induced phase noise in a DPSK system and determined how much of this noise contributes to performance degradation. In order to accomplish this he calculated the rms intensity ratio of XPM induced noise to SPM induced noise for a two channel WDM System. The BER was measured varying the OSNR of the signals at the receiver. It is reported that the XPM induced phase noise becomes as large as SPM induced phase noise in a NZ-DSF link for channel spacing less than 100 GHz. BER degradation is also observed for two channel systems as compared to a single channel system [19].

Goeger *et al.* (2004) derived a new modulation format independent method for rapid calculation of XPM impairments in multi channel WDM systems with dispersion compensation [20].

Abdul-Rashid *et al.* (2006) investigated the performance optimization in SCM-WDM Passive Optical Networks in the presence of XPM and GVD both experimentally and theoretically [21]. A general expression for electrical average noise power and electrical crosstalk level due to XPM and GVD was derived to measure the system performance for N number of WDM channels. Using the expression, they have shown that XPM and GVD causes crosstalk in the system and imposes a power penalty as the number of WDM channels increases for a given channel spacing and modulating frequency.

Sakib *et al.* (2006) have theoretically shown the impact of XPM on the performance of a WDM optical transmission system with short-period dispersion – managed fiber (SPDMF) [22]. They analyzed the performance for 2-channel WDM system using SPDMF to evaluate the impact of XPM on BER. The computed results show that the BER performance can be improved considerably by using an SPDMF.

Lee *et al.* (2007) simulated the impact of filter dispersion slope on the performance of 40 Gbps DWDM systems and networks [23]. They have proposed a novel technique which enables the separation of the performance impacts of different orders of fiber dispersion in optical fiber cascade. The technique was applied in trial optical system and networks through the use of simulation.

Yasim *et al.* (2007) theoretically studied the effect of XPM crosstalk in WDM networks on received power and number of channels for various fiber types [25]. They have presented a comprehensive theoretical study of XPM in optical fiber with exploring four fiber types. The XPM induced crosstalk noise is described by a system of coupled equations, which describes mutual channel interference optical losses in multi channel optical communications system. The corresponding system of equations has then been numerically integrated and the channels interaction phenomena such as cross-phase modulation have been described. System performance is evaluated through determining the cumulative XPM crosstalk relation with both of the received power and number of channels.

Shaari *et al.* (2008) theoretically studied the effect of XPM crosstalk in WDM networks on received power and number of channels for various fiber types [26]. The authors presented a theoretical analysis of the noise resulting from XPM in an optical WDM transmission system. Analytical approach has been used to evaluate BER performance limitation of a WDM transmission system imposed by crosstalk due to XPM and the influence of changing channel spacing for various fiber types on the BER. Numerical results demonstrated the validity of their analysis and theoretical expressions have an insight into nonlinear effect under investigation.

From the above discussion and literature review, we observed that most of the research works have addressed the problem of XPM crosstalk without or with the presence of first order GVD. No work is reported yet about the impact of XPM crosstalk considering the presence of first- and second order GVD together in a WDM system. But at high bit rate and long haul system, the second order GVD may have destructive effect on optical transmission the system. Thus, it is essential to study the impact of XPM and in presence of first- and second order GVD for predicting the performance limitation or system outage accurately due to XPM in WDM system. In this research work, an analytical model for a WDM system is developed incorporating the combined effect of XPM, first- and second order GVD. The crosstalk expression for the affected channel (called probe) is derived in terms of system parameters.

1.4 Objectives of the thesis

Signal transmission in WDM optical fiber communication system is mainly impaired and ultimately limited by GVD and XPM. GVD effect is linear in nature and present even in single channel system. XPM is a nonlinear phenomenon and becomes active only when two or more optical fields are transmitted through the fiber simultaneously. So, in a multi-channel system these two effects act simultaneously. Again, at moderately high bit rate (>10 Gbps) and first order GVD compensated system, the effect of second order GVD become significant and need to be taken into account. The main objectives of this research work are:

(i) To derive an analytical model for studying the effect of XPM in presence of first- and second orders GVD,

(ii) To find the effect of channel spacing as function of modulation frequency due to XPM,

(iii) To find the bit error rate performance as a function of input channel power, channel spacing, GVD,

(iv) To compare the above mentioned effects for different types of telecommunication grade fiber *i.e.*, SSMF, DSF and LEAF.

1.5 Thesis organization

In chapter 2, we focus on the basics of optical fiber and its properties. We also present brief description of different fiber impairments like- attenuation, linear and nonlinear effects. In chapter 3, we illustrate the analytical and simulation modeling of XPM crosstalk in presence of GVD. Results and discussion are presented in chapter 4. In chapter 5, we draw the conclusion of our work and also discuss further scope of future research.

CHAPTER 2

Optical Communication and Fiber Nonlinearities

2.1 Principles of optical communication

An optical fiber communication system is a particular type of telecommunication system, in which information to be conveyed enters an electronic transmitter. In the transmitter prepared for transmission very much in the conventional manner and it converts into electrical form, modulated and multiplexed. The signal then moves to the optical transmitter, where it is converted into optical form and the resulting light signal is transmitted over optical fiber. At the receiver end, an optical detector converts the light back into an electrical signal, which is processed by the electronic receiver to extract the information and present it in a usable form (audio, video, or data output). So a typical optical communication system consists of three major components: Optical transmitter, Optical fiber and Optical receiver as in Fig. 2.1.

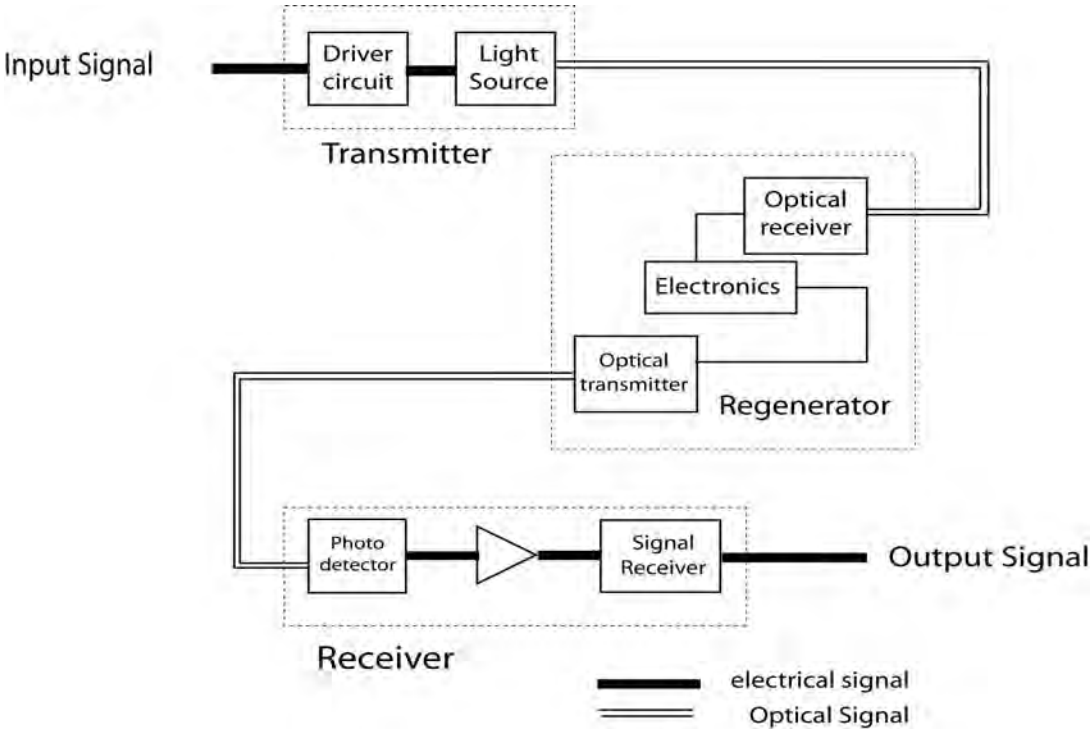

Fig. 2.1: Basic block diagram of an optical fiber communication system

2.1.1 Optical transmitter

The heart of the optical transmitter is a light source. The main function of an optical transmitter is to transform the electrical signal into optical signal using light source. The block diagram of an optical transmitter is shown in Fig. 2.2. It consists of an optical source, a modulator and a channel coupler. Semiconductor laser or light emitting diodes are used as optical source. The main consideration in selecting a source is its ability in launching maximum power into the optical fiber in the suitable wavelength. The optical signal is generated after modulating the light wave by the input signal. The coupler is generally a micro-lens that focuses the optical signal onto the entrance plane of an optical fiber with the maximum possible efficiency. The amount of launched power is an important factor in designing the optical communication system.

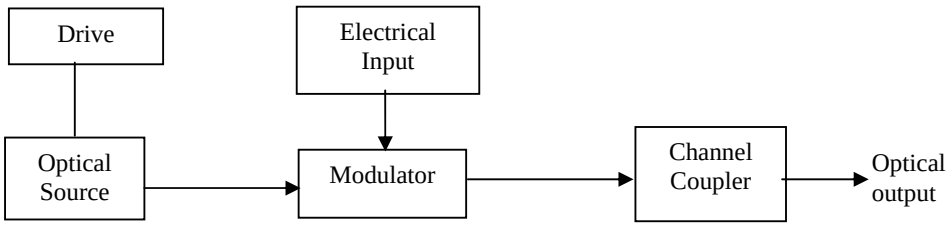

Fig. 2.2: Block diagram of an optical transmitter

2.1.2 Optical receiver

The key component of an optical receiver is its photo-detector. The main function of optical receiver is to converts the received optical signal from the fiber into the original electrical signal using photo-detector. The block diagram of an optical receiver is shown in Fig. 2.3.

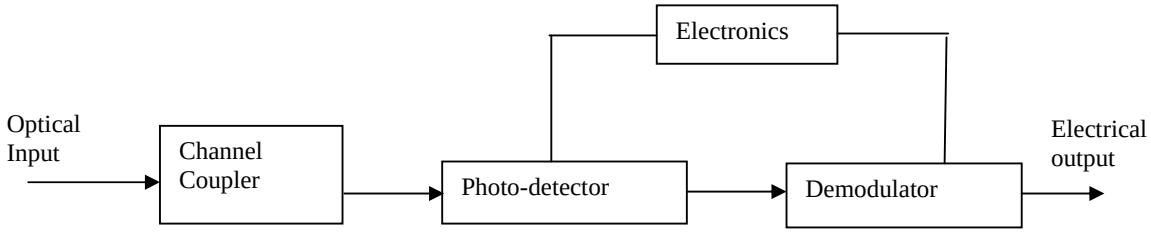

Fig. 2.3: Block diagram of an optical receiver

The optical receiver consists of a coupler, a photo-detector and a demodulator. The coupler focuses the received optical signal onto the photo-detector. Semiconductor photo diodes are used as photo-detectors because of their compatibility with the whole system. The design of the modulator depends on the modulation format used in the system. The design of the modulator depends on the modulation format used in the system. One of the most important design parameter is receiver sensitivity.

2.1.3 Optical fiber

Optical fiber is the transmission medium of the optical fiber communication system which bridge the distance between the optical transmitter and the optical receiver. To ensure the propagation of the transmitted signal up to the receiver with acceptable level of attenuation and distortion, the main consideration in designing the fiber so that the same information can be received at the receiver with minimum error. With the development in the field of optical fiber communication, the attenuation of the signal could be reduced to 0.2 dB/km. Factors that contributed to this reduction in the loss parameter improved fiber design technique, low loss fiber window, dispersion compensation, etc. Fiber loss, dispersion and nonlinear effects are main design considerations of optical fiber. Introduction of optical amplifiers and dispersion shifted fibers could successfully address the limitations imposed by fiber loss and dispersion. But many aspects of nonlinear characteristics of the fiber yet remained as the limitation of optical fibers.

2.2 Optical fiber characteristics

Optical fiber systems have many advantages over metallic based communication systems. These advantages include interference, attenuation, and bandwidth characteristics. Furthermore, the relatively smaller cross section of fiber-optic cables allows room for substantial growth of the capacity in existing conduits. Fiber-optic characteristics can be classified as linear and nonlinear. Nonlinear characteristics are influenced by parameters, such as bit rates, channel spacing and power levels.

2.2.1 Linear characteristics

Linear characteristics include attenuation, chromatic dispersion (CD), polarization mode dispersion (PMD) and optical signal-to-noise ratio (OSNR).

2.2.1.1 Attenuation

Several factors can cause attenuation, but it is generally categorized as either intrinsic or extrinsic. Intrinsic attenuation is caused by substances inherently present in the fiber, whereas extrinsic attenuation is caused by external forces such as bending. The attenuation coefficient α is expressed in decibels per kilometer and represents the loss in decibels per kilometer of fiber.

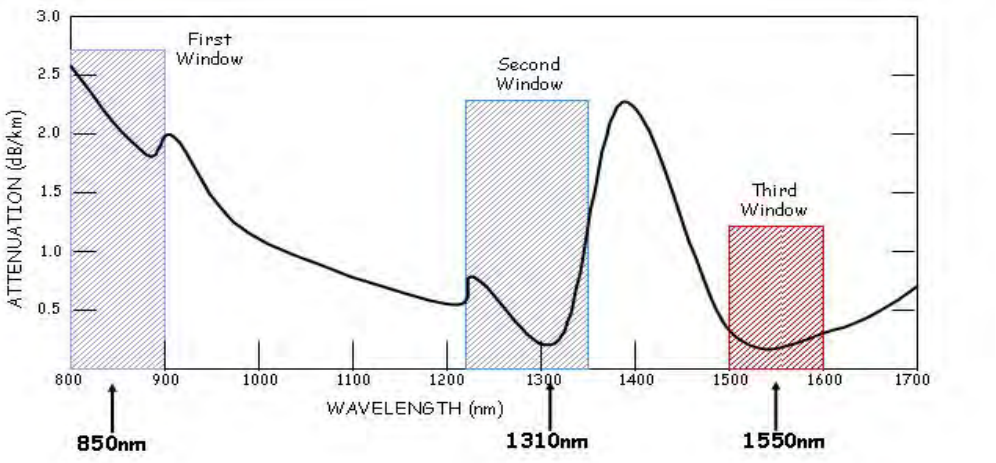

Fig. 2.4: Attenuation / loss in optical fiber

2.2.1.2 Intrinsic attenuation

Intrinsic attenuation results from materials inherent to the fiber. It is caused by impurities in the glass during the manufacturing process. As precise as manufacturing is, there is no way to eliminate all impurities. When a light signal hits an impurity in the fiber, one of two things occurs: It scatters or it is absorbed. Intrinsic loss can be further characterized by two components:

- Material absorption
- Rayleigh scattering

2.2.1.2.1 Material absorption

Material absorption occurs as a result of the imperfection and impurities in the fiber. The most common impurity is the hydroxyl (OH^-) molecule, which remains as a residue despite stringent manufacturing techniques. The three principal windows of operation include the 850 nm, 1310 nm, and 1550 nm wavelength bands. These

correspond to wavelength regions in which attenuation is low and matched to the capability of a transmitter to generate light efficiently and a receiver to carry out detection. The OH^- symbols indicate that at the 850 nm, 1310 nm, and 1550 nm wavelengths, the presence of hydroxyl radicals in the cable material causes an increase in attenuation. These radicals result from the presence of water remnants that enter the fiber-optic cable material through either a chemical reaction in the manufacturing process or as humidity in the environment.

The variation of attenuation with wavelength due to the *water peak* for standard, single-mode fiber-optic cable occurs mainly around 1380 nm. Recent advances in manufacturing have overcome the 1380 nm water peak and have resulted in zero-water-peak fiber (ZWPF). Examples of these fibers include SMF-28e from Corning and the Furukawa-Lucent OFS AllWave. Absorption accounts for 3% to 5% of fiber attenuation. This phenomenon causes a light signal to be absorbed by natural impurities in the glass and converted to vibration energy or some other form of energy such as heat. Unlike scattering, absorption can be limited by controlling the amount of impurities during the manufacturing process. Because most fiber is extremely pure, the fiber does not heat up because of absorption.

2.2.1.2.2 Rayleigh scattering

As light travels in the core, it interacts with the silica molecules in the core. Rayleigh scattering is the result of these elastic collisions between the light wave and the silica molecules in the fiber. Rayleigh scattering accounts for about 96% of attenuation in optical fiber. If the scattered light maintains an angle that supports forward travel within the core, no attenuation occurs. If the light is scattered at an angle that does not support continued forward travel, however, the light is diverted out of the core and attenuation occurs. Depending on the incident angle, some portion of the light propagates forward and the other part deviates out of the propagation path and escapes from the fiber core. Some scattered light is reflected back toward the light source. This is a property that is used in an optical time domain reflectometer (OTDR) to test fibers. The same principle applies to analyzing loss associated with localized events in the fiber, such as splices. Short wavelengths are scattered more than longer wavelengths. Any wavelength that is below 800 nm is unusable for optical communication because

attenuation due to Rayleigh scattering is high. At the same time, propagation above 1700 nm is not possible due to high losses resulting from infrared absorption.

2.2.1.3 Extrinsic attenuation

Extrinsic attenuation can be caused by two external mechanisms: macro bending or micro bending. Both cause a reduction of optical power. If a bend is imposed on an optical fiber, strain is placed on the fiber along the region that is bent. The bending strain affects the refractive index and the critical angle of the light ray in that specific area. As a result, light traveling in the core can refract out, and loss occurs. A macro bend is a large-scale bend that is visible, and the loss is generally reversible after bends are corrected. To prevent macro bends, all optical fiber has a minimum bend radius specification that should not be exceeded. This is a restriction on how much bend a fiber can withstand before experiencing problems in optical performance or mechanical reliability.

The second extrinsic cause of attenuation is a micro bend. Micro bending is caused by imperfections in the cylindrical geometry of fiber during the manufacturing process. Micro bending might be related to temperature, tensile stress, or crushing force. Like macro bending, micro bending causes a reduction of optical power in the glass. Micro bending is much localized and the bend might not be clearly visible on inspection. With bare fiber, micro bending can be reversible.

2.2.1.4 Chromatic dispersion

Chromatic dispersion is the spreading of a light pulse as it travels down a fiber. Light has a dual nature and can be considered from an electromagnetic wave as well as quantum perspective. This enables us to quantify it as waves as well as quantum particles. During the propagation of light, all of its spectral components propagate accordingly. These spectral components travel at different group velocities that lead to dispersion called GVD. Dispersion resulting from GVD is termed chromatic dispersion due to its wavelength dependence. The effect of chromatic dispersion is pulse spread.

As the pulses spread, or broaden, they tend to overlap and are no longer distinguishable by the receiver as 0s and 1s. Light pulses launched close together (high data rates) that spread too much (high dispersion) result in errors and loss of information. Chromatic dispersion occurs as a result of the range of wavelengths present

in the light source. Light from lasers and LEDs consists of a range of wavelengths, each of which travels at a slightly different speed. Over distance, the varying wavelength speeds cause the light pulse to spread in time. This is of most importance in single-mode applications. Modal dispersion is significant in multimode applications, in which the various modes of light traveling down the fiber arrive at the receiver at different times, causing a spreading effect. Chromatic dispersion is common at all bit rates. Chromatic dispersion can be compensated for or mitigated through the use of dispersion-shifted fiber (DSF). DSF is fiber doped with impurities that have negative dispersion characteristics. Chromatic dispersion is measured in ps/nm-km. A 1-dB power margin is typically reserved to account for the effects of chromatic dispersion.

When an electromagnetic wave interacts with bound electrons of a dielectric, the medium response in general depends on the optical frequency ω. This property referred to as chromatic dispersion. The chromatic dispersion parameter in a single mode fiber is the sum of the material and waveguide dispersions, so that:

$$D(\lambda) = D_{mat}(\lambda) + D_{wg}(\lambda) \qquad (2.1)$$

This relation is very important since the material dispersion parameter above 1300 nm becomes positive while the waveguide dispersion parameter stays negative. The fact is that they cancel each other out, resulting in a zero chromatic dispersion parameter D (λ) = 0. This loss is around 1310 nm, the customary operating wave for standard single mode fiber [Fig. 2.5].

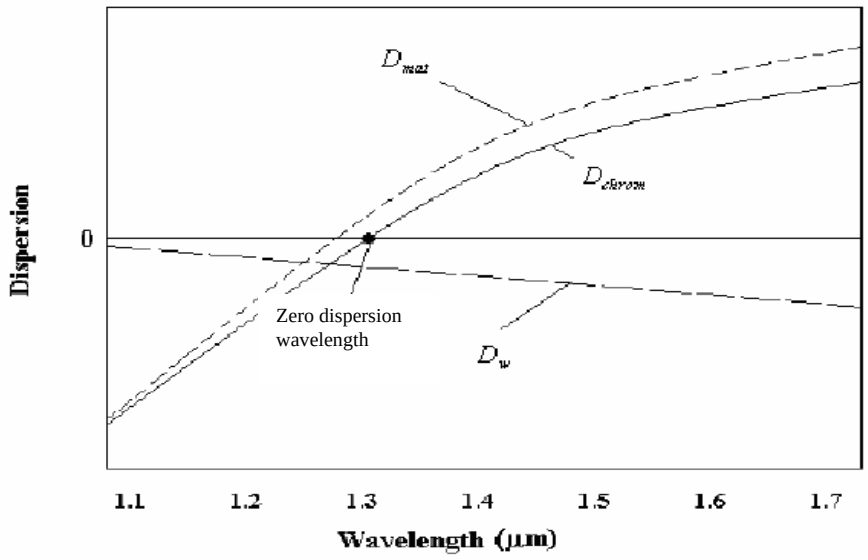

Fig. 2.5: Chromatic dispersion parameters in ps/(nm^2.km) of a standard single-mode fiber as a function of wavelength in μm.

Pulse spreading caused by chromatic dispersion,

$$\Delta t_{chrom} / L = D(\lambda)\Delta\lambda \tag{2.2}$$

Where D (λ) is the chromatic dispersion parameter of the fiber and $\Delta\lambda$ is the spectral width of the light source, as is customary. Manufacturers specify the chromatic dispersion parameter for multimode fibers either by giving its value or by giving the formula:

$$D(\lambda) = \frac{S_0}{4}\left[\lambda - \frac{\lambda_0^4}{\lambda^3}\right] \tag{2.3}$$

Where S_0 is the zero-dispersion slope in ps/(nm^2.km), λ_0 is the zero dispersion wavelength, and λ is the operating wavelength.

To calculate the dispersion parameter near the zero dispersion wavelengths, λ_0, one can use a simplified version of the above formula:

$$D(\lambda) = S_0[\lambda - \lambda_0] \tag{2.4}$$

where the zero dispersion slope, S_0 can be found in a fiber data sheet.

The dispersion parameter D is commonly used in place of β_2 to describe the total dispersion of a single mode fiber. It is related to β_2 by the relation

$$D = \frac{d\beta_1}{d\lambda} = -\frac{2\pi c}{\lambda^2}\beta_2 \tag{2.5}$$

However, chromatic dispersion is an important phenomenon in the propagation of short pulses in optical fibers. Temporally short pulses have a large spectral bandwidth. The different spectral components of the pulse travel through the medium at slightly different group velocities because of chromatic dispersion, which can result in a temporal broadening of the light pulses with no effect on their spectral compositions. This phenomenon is referred to as GVD.

2.2.1.5 Group velocity dispersion

GVD is an important effect because when a short pulse propagates through an optical fiber its pulse width gets broaden. The effects of fiber dispersion can be understood by expanding the mode- propagation constant / phase constant β in a Taylor series about the frequency ω_0 at which the pulse spectrum is centered:

$$\beta(\omega) = n(\omega)\frac{\omega}{c} = \beta_0(\omega_0) + \frac{d\beta}{d\omega}(\omega-\omega_0) + \frac{1}{2}\frac{d^2\beta}{d\omega^2}(\omega-\omega_0)^2 + \frac{1}{6}\frac{d^3\beta}{d\omega^3}(\omega-\omega_0)^3 + \cdots \tag{2.6}$$

where ω_0 is the centre frequency and β is frequency dependence, $\beta = f(\omega)$,

where $\frac{d\beta}{d\omega} = \frac{1}{v_g} = \beta_1$ = Inverse group velocity=first – order dispersion.

$\frac{d^2\beta}{d\omega^2} = \beta_2$ = First- order group velocity dispersion = 2nd order dispersion.

$\frac{d^3\beta}{d\omega^3} = \beta_3$ = Second- order group velocity dispersion = 3rd order dispersion and

$$\beta_m = \left(\frac{d^m\beta}{d\omega^m}\right)_{\omega=\omega_0} \qquad \text{(m=0, 1, 2 , 3 , . . .)} \tag{2.8}$$

The following relationship of β_0 , β_1 , β_2 and β_3 can be written in terms of refractive index (n), group velocity index (n_g) and dispersion coefficient (D) respectively.

$$\beta_0 = n(\omega_0)\frac{\omega_0}{c} \ , \tag{2.9}$$

$$\beta_1 = \frac{1}{c}\left(n + \omega\frac{dn}{d\omega}\right) = \frac{1}{v_g} = \frac{n_g}{c} \ , \tag{2.10}$$

$$\beta_2 = \frac{1}{c}\left(2\frac{dn}{d\omega} + \omega\frac{d^2n}{d\omega^2}\right) = \frac{d}{d\omega}\left(\frac{1}{v_g}\right) = -\frac{\lambda^2}{2\pi c}\cdot D \tag{2.11}$$

$$\beta_3 = \frac{d^3\beta}{d\omega^3} = \frac{d}{d\omega}\left(\frac{d^2\beta}{d\omega^2}\right) = \frac{d\lambda}{d\omega}\cdot\frac{d}{d\lambda}\left(\frac{d^2\beta}{d\omega^2}\right) = \frac{d\lambda}{d\omega}\cdot\frac{d}{d\lambda}\left(-\frac{\lambda^2}{2\pi c}\cdot D(\lambda)\right)$$

$$= \frac{1}{-\frac{2\pi c}{\lambda^2}}\cdot\frac{-2\lambda}{2\pi c}\cdot\frac{d}{d\lambda}\left[\lambda^2 D(\lambda)\right] = \frac{\lambda^3}{2\pi^2 c^2}\left[D(\lambda) + \frac{\lambda}{2}\cdot\frac{dD(\lambda)}{d\lambda}\right]$$

$$\therefore \beta_3 = \frac{\lambda^3}{2\pi^2 c^2}\left[Dispersion\_Cofficient + \frac{\lambda}{2}\cdot Dispersion\_Slope\right] \tag{2.12}$$

2.3 Fiber losses

An important fiber parameter is the measure of power loss during transmission of optical signals inside an optical fiber. If P_0 is the power launched at the input of a fiber of length L, the transmitted power P_T is given by

$$P_T = P_0 \exp(-\alpha L), \tag{2.13}$$

Where the attenuation coefficient α is a measure of overall fiber losses from all sources. It is customary to express α in units of dB/km by the relation

$$\alpha[dB/km] = -\frac{10}{L}Log_{10}\left(\frac{P_{out}}{P_{in}}\right) \approx 4.343\alpha \tag{2.14}$$

Several intrinsic and extrinsic sources contribute to the overall losses; the most important among them is Rayleigh scattering. Rayleigh scattering is the fundamental loss in optical fiber. It is referred to scattering which is the fundamental loss in optical fiber. The loss is expressed in dB/km through

$$\alpha_R = C / \lambda^4 \tag{2.15}$$

where C is a constant. Rayleigh scattering varies as a function of λ^{-4} and is the dominant loss mechanism for wavelengths shorter than 1.2 μm. The attenuation of a standard step-index single-mode fiber is about 12 dB/km near 630 nm.

2.4 Fiber types

This section discusses various multi-mode fiber (MMF) and single mode (SMF) types currently used for building premise, metro, aerial, submarine, and long-haul applications. The International Telecommunication Union (ITU-T), which is a global standardization body for telecommunication systems and vendors, has standardized various fiber types. These include the 50/125 μm graded index fiber (G.651), Non dispersion-shifted fiber (G.652), dispersion-shifted fiber (G.653), 1550-nm loss-minimized fiber (G.654), and NZDSF (G.655).

2.4.1 Multimode fiber with a 50 micron core (ITU-T G.651)

The ITU-T G.651 is an MMF with a 50 μm nominal core diameter and a 125 μm nominal cladding diameter with a graded refractive index. The attenuation parameter of G.651 fiber is 0.8 dB/km at 1310 nm. The main application for ITU-T G.651 fiber is for short-reach optical transmission systems. This fiber is optimized for use in the 1300 nm band. It can also operate in the 850 nm band and widely used in LAN application.

2.4.2 Non dispersion-shifted fiber (ITU-T G.652)

The ITU-T G.652 fiber is also known as standard SMF and is the most commonly deployed fiber. This fiber has a simple step-index structure and is optimized for operation in the 1310 nm band. It has a zero-dispersion wavelength at 1310 nm and can also operate in the 1550 nm band, but it is not optimized for this region. The typical chromatic dispersion at 1550 nm is high at 17 ps/nm-km. Dispersion compensation must

be employed for high bit rate applications. The attenuation parameter is typically 0.2 dB/km at 1550 nm and the PMD parameter is less than 0.1 ps/ km for G.652 fiber. An example of this type of fiber is Corning SMF-28.

2.4.3 Low water peak non-dispersion-shifted fiber (ITU-T G.652.C)

The legacy ITU-T G.652 standard SMFs are not optimized for WDM applications due to the high attenuation around the water peak region. ITU G.652.C-compliant fibers offer extremely low attenuation around the OH^- peaks. The G.652.C fiber is optimized for networks where transmission occurs across a broad range of wavelengths from 1285 nm to 1625 nm. Although G.652.C compliant fibers offer excellent capabilities for shorter, unamplified metro- and access networks, they do not fully address the needs for 1550 nm transmission. The attenuation parameter for G.652 fiber is typically 0.2 dB/km at 1550 nm and the PMD parameter is less than 0.15 ps/ km. An example of this type of fiber is Corning SMF-28e.

2.4.4 Dispersion-shifter fiber (ITU-T G.653)

Conventional SMF has a zero-dispersion wavelength that falls near the 1310 nm window band. SMF shows high dispersion values over the range between 1500 nm and 1600 nm (third window band). The trend of shifting the operating transmission wavelength from 1310 nm to 1550 nm initiated the development of a fiber type called *dispersion-shifted fiber (DSF)*. DSF exhibits a zero-dispersion value around 1550 nm wavelength where the attenuation is very less. The DSFs are optimized for operating in the region between 1500 to 1600 nm. With the introduction of WDM systems, however, channels allocated near 1550 nm in DSF are seriously affected by noise induced as a result of nonlinear effects caused by FWM. This initiated the development of NZDSF.

2.4.5 1550-nm loss-minimized fiber (ITU-T G.654)

The ITU-T G.654 fiber is optimized for operation in the 1500-nm to 1600-nm region. This fiber has a low loss in the 1550 nm band. Low loss is achieved by using a pure silica core. ITU-T G.654 fibers can handle higher power levels and have a larger core area. These fibers have a high chromatic dispersion at 1550 nm. The ITU G.654 fiber has been designed for extended long-haul undersea applications.

2.4.6 Nonzero dispersion shifted fiber (ITU-T G.655)

Using nonzero dispersion-shifted fiber (NZDSF) can mitigate nonlinear characteristics. NZDSF fiber overcomes these effects by moving the zero-dispersion wavelength outside the 1550 nm operating window. The practical effect of this is to have a small but finite amount of chromatic dispersion at 1550 nm, which minimizes nonlinear effects, such as FWM, SPM, and XPM, which are seen in the dense WDM systems without the need for costly dispersion compensation. There are two fiber families called nonzero dispersion (NZD+ and NZD–), in which the zero-dispersion value falls before and after the 1550-nm wavelength, respectively. The typical chromatic dispersion at 1550 nm is 4.5 ps/nm-km for G.655 fiber. The attenuation parameter for G.655 fiber is typically 0.2 dB/km at 1550 nm, and the PMD parameter is less than 0.1 ps/ km. The Corning LEAF fiber is an example of an enhanced G.655 fiber with a 32 percent larger effective area. A comparison of different types of commercial fiber discussed above is given in Table 2.1.

Table 2.1 Single Mode Fiber Standards

ITU-T Standard	**Name of the Fiber**	**Typical Attenuation value (C-band)**	**Typical CD value (C-band)**	**Applicability**
G.652	Standard single mode	0.25 dB/km	17 ps/nm-km	OK for xWDM
G.652c	Low water peak SMF	0.25 dB/km	17 ps/nm-km	Good for CWDM
G.653	Dispersion-shifted fiber	0.25 dB/km	3.5 ps/nm-km	Bad for xWDM
G.655	Non-zero dispersion-shifted fiber (NZDSF)	0.25 dB/km	4.5 ps/nm-km	Good for DWDM

2.5 Fundamentals of nonlinear effects in optical fibers

Nonlinear effects are classified into two classes: stimulated scattering and Kerr effect. Stimulated scattering depends on the threshold power. If the power carried by the fiber exceed threshold, the stimulated scattering effects become effects. There are two

types of stimulated scattering. These are: stimulated Raman scattering (SRS) and stimulated Brillouin scattering (SBS). The Kerr effect is due to the nonlinear refractive index of the core. The Kerr effects are: self-phase modulation (SPM), cross-phase modulation (XPM), four-wave mixing (FWM).

2.5.1 Stimulated Brillouin scattering (SBS)

SBS falls under the category of inelastic scattering in which the frequency of the scattered light is shifted downward. This results in the loss of the transmitted power along the fiber. At low power levels, this effect will become negligible. SBS sets a threshold on the transmitted power, above which considerable amount of power is reflected. This back reflection will make the light to reverse direction and travel towards the source. This usually happens at the connector interfaces where there is a change in the refractive index. As the power level increases, more light is backscattered since the level would have crossed the SBS threshold. The parameters which decide the threshold are the wavelength and the line width of the transmitter. Lower line width experiences lesser SBS and the increase in the spectral width of the source will reduce SBS. In case of bit streams with shorter pulse width, no SBS will occur. The value of the threshold depends on the RZ and NRZ waveforms which are used to modulate the source. It is typically 5 mW and can be increased to 10 mW by increasing the bandwidth of the carrier greater than 200 MHz by phase modulation.

SBS is due to the acoustic properties of photon interaction with the medium. When light propagates through a medium, the photons interact with silica molecules during propagation. The photons also interact with themselves and cause scattering effects such as SBS in the reverse direction of propagation along the fiber. In SBS, a low-wavelength wave called *Stoke's wave* is generated due to the scattering of energy. This wave amplifies the higher wavelengths. The gain obtained by using such a wave forms the basis of Brillouin amplification. The Brillouin gain peaks in a narrow peak near the C-band. SBS is pronounced at high bit rates and high power levels. The margin design requirement to account for SRS/SBS is 0.5 dB.

2.5.2 Stimulated Raman scattering (SRS)

When light propagates through a medium, the photons interact with silica molecules during propagation. The photons also interact with themselves and cause scattering effects, such as SRS, in the forward and reverse directions of propagation along the fiber. This results in a sporadic distribution of energy in a random direction. SRS refers to lower wavelengths pumping up the amplitude of higher wavelengths, which results in the higher wavelengths suppressing signals from the lower wavelengths. One way to mitigate the effects of SRS is to lower the input power.

In SRS, a low-wavelength wave called *Stoke's wave* is generated due to the scattering of energy. This wave amplifies the higher wavelengths. The gain obtained by using such a wave forms the basis of Raman amplification. The Raman gain can extend most of the operating band (C- and L-band) for WDM networks. SRS is pronounced at high bit rates and high power levels. The margin design requirement to account for SRS/SBS is 0.5 dB. A comparison of SRS and SBS effect is given in Table2.2

Table 2.2 Comparison between SBS and SRS Properties

Property	**SBS**	**SRS**
Direction of scatter	Only in backward direction	In both forward and backward direction
Frequency shift	About 10 GHz	About 13 THz
Spectrum width	Narrow width	Broad spectrum width

2.5.3 Optical Kerr effect

The Kerr effect, also called the quadratic electro-optic effect (QEO effect), is a change in the refractive index of a material in response to an applied electric field.The Kerr effect was discovered in 1875 by John Kerr, a Scottish physicist. The optical Kerr effect, or AC Kerr effect is the case in which the electric field is due to the light itself. This causes a variation in index of refraction which is proportional to the local irradiance of the light. This refractive index variation is responsible for the nonlinear optical effects of self-focusing, self-phase modulation and modulational instability, and is the basis for Kerr-lens modelocking. This effect only becomes significant with very intense beams such as those from lasers.

2.5.3.1 Self-phase modulation (SPM)

Phase modulation of an optical signal by itself is known as *self-phase modulation (SPM).* SPM is primarily due to the self-modulation of the pulses. The nonlinear phase shift of the optical carrier signal change with respect to time because pulse intensity (power) changes over time. Generally, SPM occurs in single-wavelength systems. At high bit rates, however, SPM tends to cancel dispersion. SPM increases with high signal power levels. In fiber plant design, a strong input signal helps overcome linear attenuation and dispersion losses. However, consideration must be given to receiver saturation and to nonlinear effects such as SPM, which occurs with high signal levels. SPM results in phase shift and a nonlinear pulse spread. As the pulses spread, they tend to overlap and are no longer distinguishable by the receiver. The damaging effect due SPM depends on power transmitted, the length of the link and bit rate. The acceptable norm in system design to counter the SPM effect is to take into account a power penalty that can be assumed equal to the negative effect posed by XPM. A 0.5-dB power margin is typically reserved to account for the effects of SPM at high bit rates and power levels. Pulse broadening due to SPM is shown in Fig. 2.6.

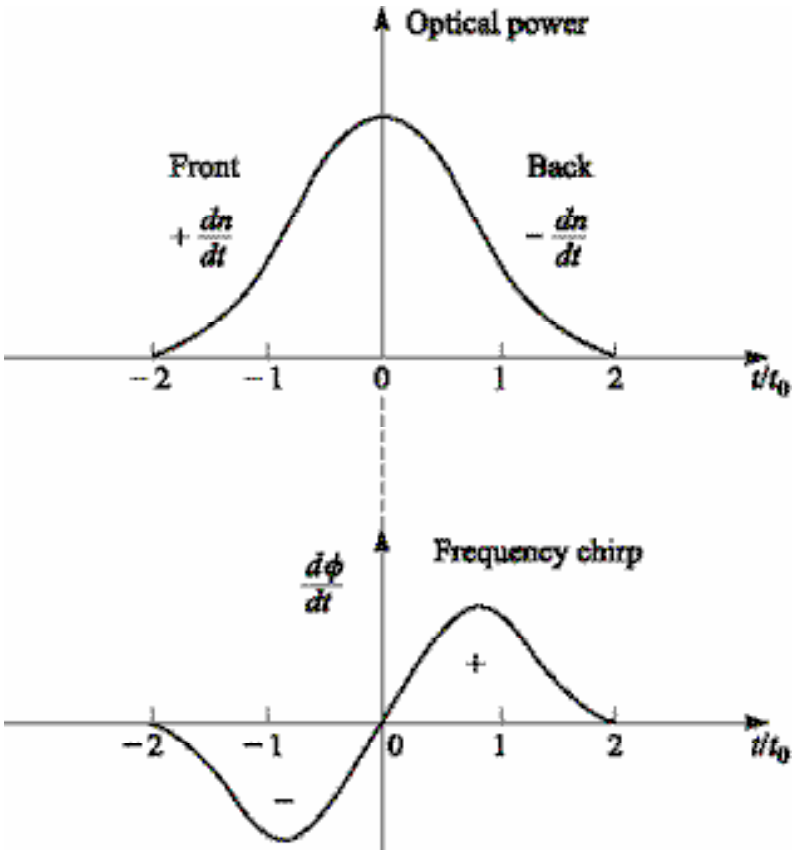

Fig. 2.6: Phenomenological description of spectral broadening of pulse due to SPM.

2.5.3.2 Cross- phase modulation (XPM)

Another nonlinear phase shift originating from the Kerr effect is cross-phase modulation (XPM). While SPM is the effect of a pulse on its own phase, XPM is a nonlinear phase effect due to optical pulses in neighboring channels. Therefore, XPM occurs only in multi-channel systems. In a multi-channel system, the nonlinear phase shift of the signal at the center wavelength λ_i is described by [25],

$$\phi_{NL} = \frac{2\pi}{\lambda_i} n_2 z \left[I_i(t) + 2\sum_{i \neq j}^{M} I_j(t) \right] \tag{2.16}$$

Where M is the number of co-propagating channels in the fiber. The first term is responsible for SPM and the second term is for XPM. Equation (2.1) might lead to a speculation that the effect of XPM could be at least twice as significant as that of SPM. XPM is a nonlinear effect that limits system performance in WDM systems. XPM is the phase modulation of a signal caused by an adjacent signal within the same fiber. XPM is related to the combination (dispersion/effective area). XPM results from the different carrier frequencies of independent channels, including the associated phase shifts on one another. The induced phase shift is due to the *walkover* effect, whereby two pulses at different bit rates or with different group velocities walk across each other. As a result, the slower pulse sees the walkover and induces a phase shift. The total phase shift depends on the net power of all the channels and on the bit output of the channels. Maximum phase shift is produced when bits belonging to high-powered adjacent channels walk across each other.

XPM can be mitigated by carefully selecting unequal bit rates for adjacent WDM channels. XPM, in particular, is severe in long-haul WDM networks and the acceptable norm in system design to counter XPM effect is to take into account a power penalty that can be assumed equal to the negative effect posed by XPM. However, XPM is effective only when pulses in the other channels are synchronized with the signal of interest. When pulses in each channel travel at different group velocities due to dispersion, the pulses slide past each other while propagating. Fig. 2.7 illustrates how two isolated pulses in different channels collide with each other.

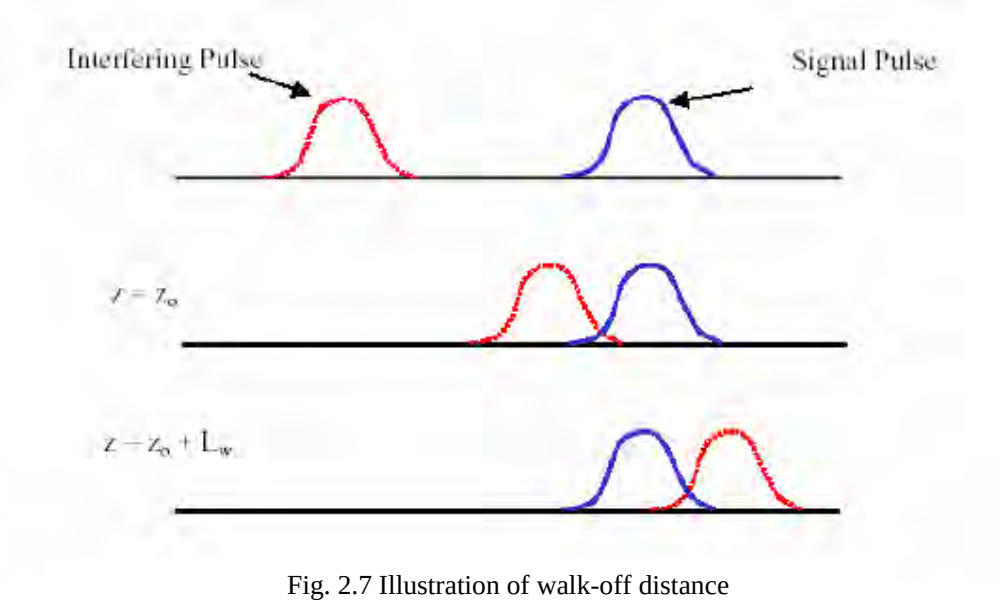

Fig. 2.7 Illustration of walk-off distance

When the faster traveling pulse has completely walked through the slower traveling pulse, the XPM effect becomes negligible. The relative transmission distance for two pulses in different channels to collide with each other is called walk-off distance, L_W [27].

$$L_W = \frac{T_0}{v_g'(\lambda_1) - v_g'(\lambda_2)} \approx \frac{T_0}{|D\Delta\lambda|} \tag{2.17}$$

where T_0 is the pulse width, v_g is the group velocity, and λ_1 , λ_2 are the center wavelength of the two channels. D is the dispersion coefficient and $\Delta\lambda = |\lambda_1 - \lambda_2|$. When dispersion is significant, the walk-off distance is relatively short and the interaction between the pulses will not be significant, which leads to a reduced effect of XPM. However, the spectrum broadened due to XPM will induce more significant distortion of temporal shape of the pulse when large dispersion is present, which makes the effect of dispersion on XPM complicated.

2.5.3.3 Four-wave mixing (FWM)

FWM can be compared to the inter-modulation distortion in standard electrical systems. When three wavelengths (λ_1, λ_2, and λ_3) interact in a nonlinear medium, they give rise to a fourth wavelength (λ_4), which is formed by the scattering of the three incident photons, producing the fourth photon. This effect is known as *four-wave mixing (FWM)* and is a fiber-optic characteristic that affects WDM systems.

The effects of FWM are pronounced with decreased channel spacing of wavelengths and at high signal power levels. High chromatic dispersion also increases FWM effects. FWM also causes inter-channel cross-talk effects for equally spaced WDM channels. FWM can be mitigated by using uneven channel spacing in WDM systems or nonzero dispersion-shifted fiber (NZDSF). A 0.5-dB power margin is typically reserved to account for the effects of FWM in WDM systems. Pictorial diagram of FWM are shown in Fig. 2.8. Table 2.3 gives a comparison of the Kerr effect.

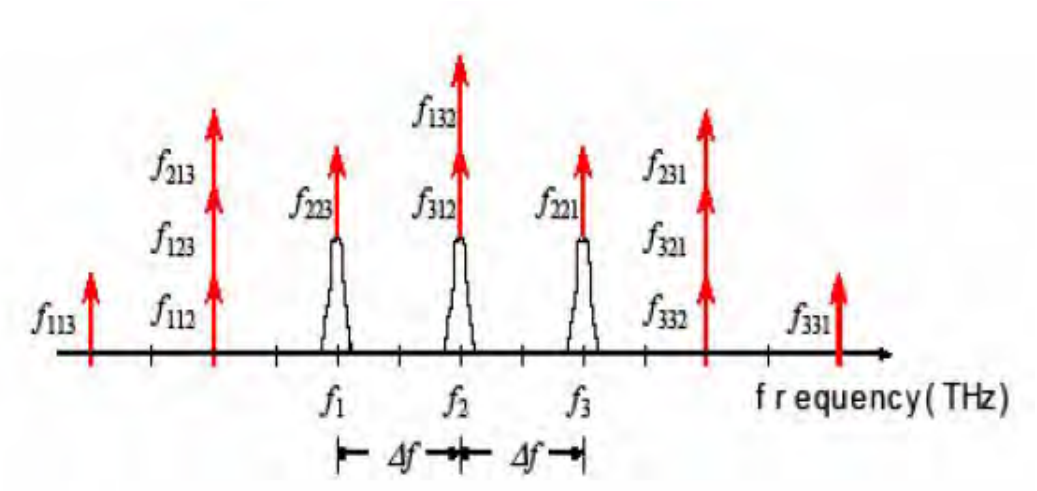

Fig. 2.8 Four-wave mixing with three injected waves at frequencies f_1 ,f_2 and f_3 and the generated frequencies are f_{ijk}

Table 2.3: Fiber nonlinearities

Characteristics	**Nonlinear Phenomenon**		
	SPM	**XPM**	**FWM**
1. Bit rate	Dependent	Dependent	Independent
2. Origin	Nonlinear susceptibility	Nonlinear susceptibility	Nonlinear susceptibility
3. Effect of X	Phase shift due pulse itself only	Phase shift is alone due to co-propagating Signal	New waves are generated
4. Shape of broadening	Symmetrical	May be symmetrical	No broadening effect
5. Channel spacing	No effect	Increases on decreasing the spacing	Increases on decreasing the spacing

2.6 Wavelength division multiplexing (WDM)

In fiber-optic communications, wavelength-division multiplexing (WDM) is a technology which multiplexes multiple optical carrier signals on a single optical fiber by using different wavelengths (colours) of laser light to carry different signals. This allows for a multiplication in capacity, in addition to enabling bidirectional communications over one strand of fiber. This is a form of frequency division multiplexing (FDM) but is commonly called WDM.

Optical transmission is becoming a preferred medium for long-distance, high-bandwidth communication systems running at speeds in the range of gigabits per second (Gb/s) or higher. The progress towards ever increasing speeds encounters an obstacle in the form of the GVD or chromatic dispersion in the optical fiber that restricts bit rates. On the other hand, the progress towards longer lengths of transmission has led to increasing input powers. Nonlinear effects that depend on the Kerr coefficient then become important, especially the SPM and XPM. The use of EDFA in optical transmission systems has substantially increased the maximum length of repeaterless transmission. However, these amplifiers introduce the amplified spontaneous emission that could become a main limiter of the system performance. In addition, the optical fiber provides large amounts of bandwidths. To utilize fully these bandwidths, WDM systems have been widely proposed as a solution.

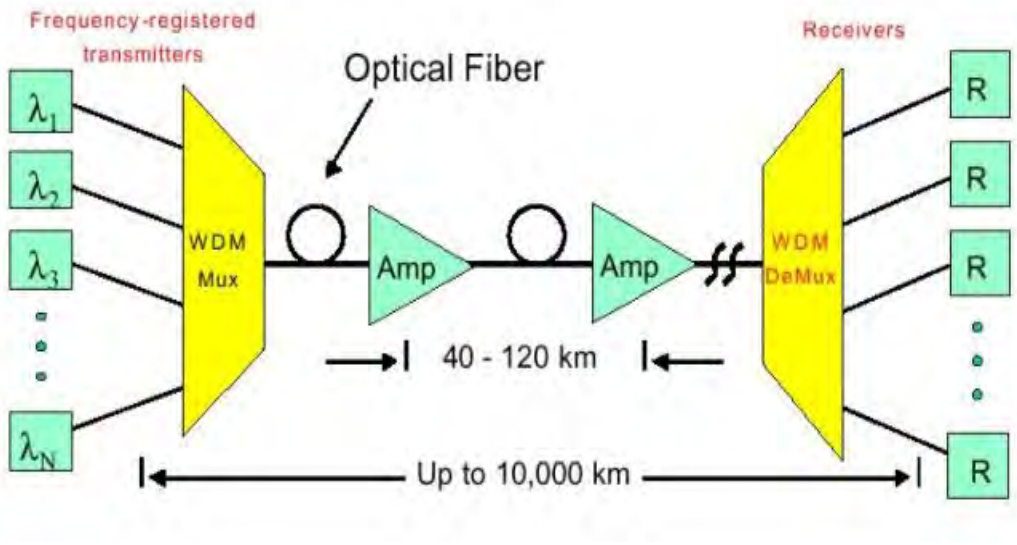

Fig. 2.9: Graphical representation of a point to point WDM optical system.

However, due to the chromatic dispersion of the fibre, the baud rate for a single optical channel eventually reached its limit. Furthermore, the transformation from the existing network, the 2.5 Gbps (OC-48 or STM16) transmission system, to the 10 Gbps (OC-194 or STM64) would prove costly seeing that the transmitting and receiving terminal of the network would have to be replaced. An important technique of super-imposing numerous wavelengths on a single fiber was thus suggested. This multiple wavelength system is referred to as WDM systems. The WDM systems proved to be economically viable because it is less expensive to update the terminal equipment of WDM than it is to install new fiber cables with the aim to increase system capacity. However, transmission on long-haul fiber was inefficient because regeneration of WDM signals implied that an optical-to-electrical conversion of the signal must be performed. This is followed by the electrical amplification of each wavelength separately and finally an electrical-to-optical conversion is performed prior to the multiplexing of the signal that is required for re-transmission of the signal. This limitation was alleviated with the inception of the EDFA. The EDFA with gain spectrum ranging from 1525-1560 nm and typical gain range of 25 -50 dB.

Block diagram of a WDM optical system is shown in Fig. 2.9. The essential components of a WDM system include a tunable laser used at the transmitting side of the system to generate the different wavelengths. Wavelength multiplexer and demultiplexers are used to combine and separate channels in and out of the fiber respectively. A post-amplifier is used to counteract the insertion loss of the multiplexer at the transmitter. Similarly, a pre-amplifier is used to increase the sensitivity of the receiver. It is also customary to include an in-line amplifier to cater for the attenuation of the fiber. As for any other system, it is important that the system is transparent. In order to do so, international standard organizations such as (ITU-T) define standard wavelength channels for optical systems. A common standard is the laser wavelength spacing of 100 GHz between channels. This standard applies to systems that use 4, 8, 16 or 32 channels. In order to gain a better understanding of WDM systems, one needs to consider the functionality of each component in the system.

CHAPTER 3

Analytical and Simulation Modeling

3.1 Introduction

The field of nonlinear optics is complex and encompasses myriads of interesting effects and practical applications. In spite of its richness most of effects can be described accurately with just a few equations. This introduction to nonlinear optics is therefore limited to a simple analysis of Maxwell's equations which govern the propagation of light.

In dielectric media and in absence of free charges or currents the Maxwell's equations are given by

$$\nabla . D(r,t) = 0 \tag{3.1}$$

$$\nabla . B(r,t) = 0 \tag{3.2}$$

$$\nabla \mathrm{X}\, E(r,t) = -\frac{\partial \mathrm{B(r,t)}}{\partial \mathrm{t}} \tag{3.3}$$

$$\nabla \mathrm{X\, H}(r,t) = -\frac{\partial \mathrm{D(r,t)}}{\partial \mathrm{t}} \tag{3.4}$$

where D is the electric displacement and B,E are the magnetic and electric fields respectively. H and D are related to the magnetic and electric fields according to

$$B(r,t) = \mu_0 H(r,t) \qquad\qquad D(r,t) = \varepsilon_0 E(r,t) + P(r,t) \tag{3.5}$$

where P is the polarization and μ_0, ε_0 are the permeability and permittivity of free space respectively. Equation (3.1) – (3.5) can be decouple and, by assuming $\nabla . \mathrm{E} = 0$, the following expression is obtained

$$-\nabla^2 E(r,t) + \frac{1}{c^2}\frac{\partial^2 E(r,t)}{\partial^2 t} = -\mu_0 \frac{\partial^2 P(r,t)}{\partial t^2} \tag{3.6}$$

where c is the speed of light in vacuum. The polarization is given by

$$P(r,t) = \varepsilon_0 \chi E(r,t) \tag{3.7}$$

where χ is the optical susceptibility. χ can be calculated by an iterative procedure employing first order perturbation methods and the polarization is therefore conveniently expressed as a sum of a linear term and nonlinear terms

$$P = P_l + P_{nl} = \varepsilon_0 \chi^{(1)} . E + \varepsilon_0 \sum_{j>2} \chi^{(j)} E^{(j)} \tag{3.8}$$

Introducing the linear refractive index $n^2(\omega) = \varepsilon(\omega) = 1 + \chi^{(1)}$, equation 3.6 can be written as

$$-\nabla^2 E(r,t) + \frac{n(\omega)^2}{c^2}\frac{\partial^2 E(r,t)}{\partial^2 t} = -\mu_0 \frac{\partial^2 P_{nl}(r,t)}{\partial t^2} \tag{3.9}$$

where $\varepsilon(\omega)$ is the dielectric function. This expression shows that the nonlinear polarization acts as a source term for a driven wave equation. In absence of P_{nl} the radiation simply propagates as a free wave with speed $v = c/n$. The only significant nonlinear contribution is there fore from $\chi^{(3)}$ .The nonlinear polarization is then reduced to

$$P_{nl}(r,t) = \varepsilon_0 \int\int\int_{-\infty}^{\infty} \chi^{(3)}(t,t_1,t_2,t_3) E(r,t_1) E(r,t_2) E(r,t_3) dt_1 dt_2 dt_3 \tag{3.10}$$

3.2 System model

The block diagram of a multi span multi channel WDM system with EDFA in cascade used for theoretical analysis is shown in Fig. 3.1. The N channels are multiplexed by WDM MUX and the composite signal is transmitted through an optical fiber. To describe the effect XPM, we assume that one channel is probe which is operated at 1559 nm wavelength is a low power continuous wave and the remaining channels are pump. The in-line EDFA's are used in cascade to compensate the fiber losses. Finally, the composite signal is demultiplexed at WDM DEMUX and from the modulated carrier, original signal is recovered through IM-DD method.

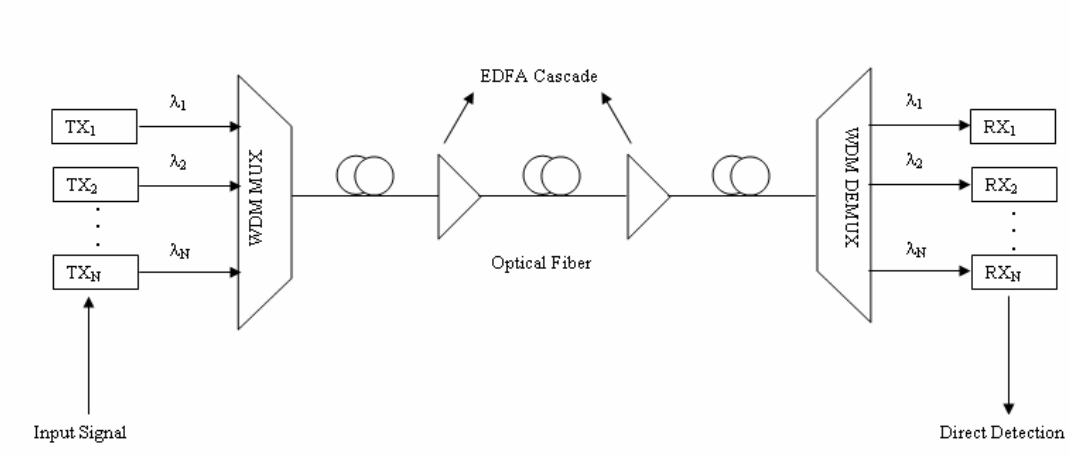

Fig. 3.1: Block diagram of a WDM system with EDFA in cascade

3.3 Pump-probe propagation equation and crosstalk

Using the slowly-varying envelope approximation, the propagation of the channels along the transmission medium is governed by the nonlinear Schrödinger equation (NLS). For this analysis, we consider only the attenuation factor, the first– and second-order GVD, as well as the SPM and XPM effects in the NLS equation given for an arbitrary channel k as follows:

$$\frac{\partial A_k}{\partial z} + \frac{\alpha_k}{2} A_k + \frac{1}{v_{gk}} \cdot \frac{\partial A_k}{\partial t} + \frac{i}{2} \beta_{2k} \frac{\partial^2 A_k}{\partial t^2} - \frac{1}{6} \beta_{3k} \frac{\partial^3 A_k}{\partial t^3} = i\gamma_k \left[|A_k|^2 + 2 \sum_{j=1, j \neq k}^{N} |A_k|^2 \right] A_{k,} \quad (3.11)$$

where *k* is the current channel under consideration, *N* is the total number of channels, α_k represents the attenuation parameter, β_{2k} and β_{3k} are the first -and second-order GVD parameter, respectively, γ_k is the nonlinearity coefficient and v_{jk} is the group velocity.

The first two terms on the right-hand side of Eq. (3.11) are the nonlinearity factors that arise due to the nonlinear refractive index of the fiber. The XPM effect is modeled in the same way as the SPM effect by introducing another term on the nonlinear part of the NLS equation. This term sums the effect of the XPM caused by all other channels. The effective nonlinear refractive index n_2 of the XPM effect is twice that of the SPM effect. This leads to a factor of 2 applied to the magnitude of the sum.

In order to simplify the analysis and focus our attention on the effect of XPM induced inter channel crosstalk, we neglect the interaction between SPM and XPM and assume that these two act independently. We will assume that the probe signal is operated in continuous wave (CW), whereas the pump signal is modulated with a sinusoidal wave at a frequency Ω. Although the effect of SPM for both the probe and the pump channels are neglected in this XPM calculation, a complete system performance evaluation must take into account the effect of SPM and other nonlinear effects separately. This approximation is valid as long as the pump signal waveform is not appreciably changed by the SPM induced distortion before its optical power is significantly reduced by the fiber attenuation. Using the substitutions $T=t-z/v_k$ and $\alpha_k = \alpha$

$$A_k(t, z) = E_k(T, z) \exp(-\alpha z / 2) \quad (3.12)$$

we have,

$$\frac{\partial E_k(T,z)}{\partial z} = -\frac{i\beta_{2k}}{2}\frac{\partial^2 E_k(T,z)}{\partial T^2} + \frac{\beta_{3k}}{6}\frac{\partial^3 E_k(T,z)}{\partial T^3} + i\gamma_k 2p_k(T - d_{jkz},0).\exp(-\alpha z)E_k(T,z) \quad (3.13)$$

where $d_{jk} \equiv (1/v_j) - (1/v_k)$ is the relative walk-off between the probe and the pump. Using a linear approximation, the walk-off d_{jk} can be expressed as $d_{jk} = D\Delta\lambda_{jk}$, where $D = -(2\pi c/\lambda^2)\beta_{2k}$ is the dispersion coefficient and second order GVD, $\beta_3 = \frac{\lambda^3}{2\pi^2 c^2}\left[D(\lambda) + \frac{\lambda}{2}.dispersion\ \ Slope\right]$, $\Delta\lambda_{jk}$ and λ are the wavelength spacing and the average wavelength between the probe and pump, respectively, and c is the light velocity. Here a linear approximation is used for d_{jk} for simplicity.

In general, dispersion and non-linearity act together along the fiber. However, in an infinitesimal fiber section dz, it can be assumed that dispersive and non-linear effects act independently, the same idea as used in the split-step Fourier method for solving the NSL equation. Substituting $E_k = |E_k|\exp[i\Phi_k(T,z)]$ in equation (3.13) gives

$$d\phi_k(T,z') = i\gamma_k 2P_j(T + d_{jk}z',0)\exp(-\alpha z')dz \quad (3.14)$$

The Fourier transformation of this phase variation gives

$$d\phi_k(\Omega,z') = i\gamma_k 2P_j(\Omega,0)e^{(-\alpha + i\Omega d_{jk})z'}dz \quad (3.15)$$

Neglecting the intensity fluctuations of the probe channel, this phase change corresponds to change in electrical field,

$$|E_k|\exp[id\phi_k(T,z')] \approx |E_k|[1 + id\Phi(T,z')] \quad (3.15a)$$

or in Fourier domain

$$|E_k|\exp[id\phi_k(\Omega,z')] \approx |E_k|[1 + id\Phi(\Omega,z')] \quad (3.15b)$$

Due to chromatic dispersion of the fiber, this phase variation generated at z=z' is converted into an amplitude variation at the end of the fiber z=L. Taking into account only the dispersion and source term of the phase perturbation at z=z', the Fourier transform of equation (3.13) becomes

$$\frac{\partial E_k(\Omega,z)}{\partial z} = -\frac{i\beta_{2k}\Omega^2}{2}E_k(\Omega,z) - \frac{\beta_{3k}\Omega^3}{6}E_k(\Omega,z) + |E_k|[1 + id\Phi(\Omega,z')]\delta(z - z') \quad (3.16)$$

Where the Kronecker delta $\delta(z - z')$ is introduced to take into account the fact the source term exists only in the infinitesimal fiber section at z=z'. Therefore at z=L the probe field becomes

$$E_k(\Omega,L)=E_k+id\Phi_k(\Omega,z')E_k\exp\left[\left(\frac{i\beta_{2k}\Omega^2}{2}-\frac{\beta_{3k}\Omega^3}{6}\right)(L-z')\right] \quad (3.17)$$

The optical power variation caused by non-linear phase modulation created in the short section dz at z=z' is thus

$$\Delta a_{jk}(\Omega.z',L)=\left|E_k(\Omega,L)\right|^2-E_k^2=-2E_k^2 d\Phi_k(\Omega,z')\sin\left[\left(\frac{\beta_{2k}\Omega^2}{2}+\frac{i\beta_{3k}\Omega^3}{6}\right)(L-z')\right] \quad (3.18)$$

where linearization has been made considering that $d\phi_k$ is infinitesimal.

Using $E_k(T,z)=A_k(T+z/v_k,z)\exp(\alpha z/2)$ and equation (3.15) and integrating all self phase modulation and cross phase modulation contributions along the fiber, gives the total intensity fluctuations at the end of the fiber.

$$\Delta s_{jk}(\Omega,L)=-4\gamma_k E_k^2\exp(-(\alpha-i\Omega/v_k)L).\int_0^L P_j(\Omega,0).Sin\left[(\beta_{2k}\Omega^2/2+i\beta_{3k}\Omega^3/6)(L-z')\right] \quad (3.19)$$
$$\exp(-(\alpha-i\Omega d_{jk})z')dz'\exp(-(\alpha-i\Omega d_{jk})z')dz'$$

Where $P_k=|A_k|^2$ and $\Delta s_{jk}(\Omega,L)=\Delta a_{jk}(\Omega,L)e^{-\alpha L}$ represents fluctuations of A_k .Which on integration gives

$$\Delta s_{jk}(\Omega,L)=2\gamma_k P_k(L)e^{i\Omega L/v_k}\left\{\frac{\exp(i\beta_{2k}\Omega^2L/2+\beta_{3k}\Omega^3L/6)-\exp(-\alpha+i\Omega d_{jk})L}{i(\alpha-i\Omega d_{jk}-i\beta_{2k}\Omega^2/2-\beta_{3k}\Omega^3/6}\right\} \quad (3.20)$$
$$-2\gamma_k P_k(L)e^{i\Omega L/v_k}\left\{\frac{\exp(-i\beta_{2k}\Omega^2L/2-\beta_{3k}\Omega^3L/6)-\exp(-\alpha+i\Omega d_{jk})L}{i(\alpha-i\Omega d_{jk}-i\beta_{2k}\Omega^2/2-\beta_{3k}\Omega^3/6}\right\}$$

where $P_k(0)$ and $P_k(L)$ are probe optical power at input and output of the fiber. Under the assumption that $\exp(-\alpha z)<<1$ and that modulation bandwidth is much smaller than the channel spacing, ie, $d_{jk}>>\beta_{2k}\Omega/2$ gives a simpler frequency domain description of the intensity fluctuations in the probe channel by the pump channel.

$$\Delta s_{jk}(\Omega,L)=4\gamma_k P_k(L)P_j(\Omega,0).\exp(i\Omega L/v_k).\frac{\sin(\beta_{2k}\Omega^2L/2+\beta_{3k}\Omega^3L/6)}{\alpha-i\Omega d_{jk}} \quad (3.21)$$

equation (3.21) cab be generalized to analyze multispan optically amplified systems, where the total intensity fluctuation at the receiver is the accumulation of XPM contributions created by each fiber span. For a system having a total of N amplified fiber spans, the XPM created in the *m*th span produces an intensity modulation $\Delta s_{jk}^{(m)}(\Omega,L_N)$ at the end of the system. Even through the phase modulation creation depends only on the pump power and the walk-off within the *m*th span, the phase-to-

intensity conversion depends on the accumulated dispersion of the fibers from the m th to the N th spans. There fore, we have

$$\Delta s_{jk}^{(m)}(\Omega, L_N) = 4\gamma_k P_k(L_N) P_j^{(m)}(\Omega,0).\exp\left[i\Omega \sum_{n=1}^{m-1} d_{jk}^{(n)} L^{(n)} \right] \cdot \frac{\sin\left[(\Omega^2 \sum_{n=m}^{N} \beta_2^{(n)} L^{(n)})/2 + (\Omega^3 \sum_{n=m}^{N} \beta_3^{(n)} L^{(n)})/6 \right]}{\alpha - i\Omega d_{jk}^{i}} \cdot \exp(i\Omega L_N / v_k) \quad (3.22)$$

where $L_N = \sum_{n=1}^{N} L^{(n)}$ is the total fiber length in the system, $L^{(m)}$ and β_2^m are the fiber length and the dispersion of the *m*th span [where $L^{(0)} = 0$], $p_k^{(m)}(\Omega,0)$ is the pump signal input power spectrum in the *m*th span and $d_{jk}^{(m)}$ is the relative walk-off between two channels in the *m*th span, [where $d_{jk}^{(0)} = 0$]. To generalize (3.21) to (3.22), the term $\sin(\beta_{2k}\Omega^2 L/2 + \beta_{3k}\Omega^3 L/6)$ in (11) is replaced by $\sin\left[(\Omega^2 \sum_{n=m}^{N} \beta_2^{(n)} L^{(n)})/2 + (\Omega^3 \sum_{n=m}^{N} \beta_3^{(n)} L^{(n)})/6 \right]$ in (3.22) to take into account the linear accumulation of dispersion, is that the pump and prove waves travel at different speeds. The phase difference between the pump and the probe waves at the input of the mth span is different from that at the input of the first span. The walk-off dependent term $\exp\left[i\Omega \sum_{n=1}^{m-1} d_{jk}^{(n)} L^{(n)} \right]$ in (3.22) takes into account the walk-off between the probe and the pump channels before they both enter into the *m*th fiber span.

Finally, contributions from all fiber spans add up and therefore, the intensity fluctuation induced by the cross-phase modulation of the whole system can be expressed as

$$\Delta s_{jk}(\Omega, L_N) = \sum_{m=1}^{N} \Delta s_k^{(m)}(\Omega, L_N) \quad (3.23)$$

In the time domain, the probe output optical power with XPM induced crosstalk is,

$$P_{jk}(t, L_N) = p_k(L_N) + \Delta s_{jk}(t, L_N) \quad (3.24)$$

$\Delta s_{jk}(t, L_N)$ is the inverse Fourier transform of $\Delta s_{jk}(\Omega, L_N)$ and $p_k(L_N)$ is the probe output without XPM. After the square law detection of photo diode, the electrical power

spectral density is the Fourier transform of the correlation of the time domain optical intensity waveform. Therefore,

$$P_k(\Omega, L_N) = \eta^2 \left\lfloor P_k^2(L_N)\delta(\Omega) + \left|\Delta s_{jk}(\Omega, L_N)\right|^2 \right\rfloor \tag{3.25}$$

where η is the photodiode responsivity.

For Ω > 0, the XPM induced electrical power spectral density in the probe channel, normalized to its power level without this effect can be expressed as

$$\Delta P_{jk}(\Omega, L_N) = \frac{\eta^2 \left|\Delta s_{jk}(\Omega, L_N)\right|^2}{\eta^2 P_k^2(L_N)} \tag{3.26}$$

$\Delta P_{jk}(\Omega, L_N)$ is defined as the normalized XPM power transfer function.

$$\Delta P_{jk}(\Omega, L_N) = \left| \sum_{i=1}^{N} \left\{ 4\gamma_k P_j^i(\Omega, 0) \exp\left[i\Omega \sum_{n=1}^{i-1} d_{jk}^{(n)} L^{(n)} \right] \cdot \frac{\sin\left(\Omega^2 \sum_{n=i}^{N} \beta_{2k}^{(n)} L^{(n)} / 2 + \Omega^3 \sum_{n=i}^{N} \beta_{3k}^{(n)} L^{(n)} / 6\right)}{\alpha - i\Omega d_{jk}^i} \right\} \right|^2 \tag{3.27}$$

which is the final expression. It is worth mentioning here that in the derivation of (3.27), we have neglected the intensity fluctuation of the probe signal before it reaches the end of the system.

3.4 Bit error rate (BER)

Optical receivers convert incident optical power into electric current through a photodiode. Among a group of optical receivers, a receiver is said to to be more sensitive if it achieves the same performance with less optical power incident on it. The communications system performance is characterized by a quantity called the bit error rate (BER) which is defined as the average probability of incorrect bit identification of a bit by the decision circuit of the receiver. For example, a BER of $2\text{x}10^{-6}$ would correspond to on average 2 errors per million bits. A commonly used criterion for digital optical receivers requires BER $\leq$ $1\text{x}10^{-9}$. It is important for the signal to have minimum distortions in order to avoid a high BER at the receiver. This means that although the combined effects of GVD, SPM and XPM cannot be eliminated they need to be reduced so that the pulse can propagate with minimum distortions. Also the inevitable presence of amplifier noises can also cause pulse distortions and hence cause system degradation. In order to assess the system performance one needs to know how

to calculate the BER of the system at the receiver end. In this chapter we calculate the BER of the system at the receiver in the presence of amplifier noises.

In any communication system the BER is the most important factor. A standard BER in communication system some times is maintained. For video, speech, data and for every information the separate BER is maintained. BER is related to the Input signal power and also SNR. As the input signal power is increases the BER decreases.

$$BER = \frac{Number\ of\ bits\ receiver\ with\ error}{Total\ number\ of\ bits} \tag{3.28}$$

Fig. 3.2 shows schematically the fluctuating signal received by the decision circuit, which samples it at the decision instant t_D determined through clock recovery. The sampled value I fluctuates from bit to bit around an average value I_1 or I_0, depending on whether the bit corresponds to 1 or 0 in the bit stream. The decision circuit compares the sampled value with the threshold value I_D and calls it bit 1 if $I > I_D$ or bit 0 if $I < I_D$.

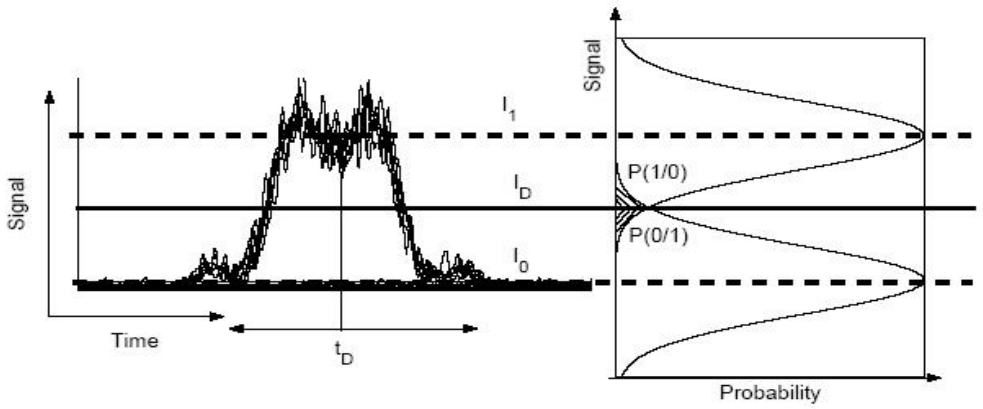

Fig. 3.2: Bit error probabilities

An error occurs if $I < I_D$ for bit 1 or if $I > I_D$ for bit 0 due to amplifier noises that add into the signal in the system. Both sources of errors can be included by defining the error probability as

$$BER = p(1)P(1/0) + p(0)P(0/1); \tag{3.29}$$

where p(1) and p(0) are the probabilities of receiving bits 1 and 0, respectively, P(0/1) is the probability of deciding 0 when 1 is received, and P(1/0) is the probability of deciding 1 when 0 is received. Since 1 and 0 bits are equally likely to occur, then we can assume, $p(1) = p(0) = 1/2$, and the BER becomes

$$BER = 1/2[P(1/0)+P(0/1)] \tag{3.30}$$

Fig. 3.2 shows how P(0/1) and P(1/0) depend on the probability density function p(I) of the sampled value I. The functional form of p(I) depends on the statistics of noise sources responsible for current fluctuations. Assuming a Gaussian noise profile, one can write the functional form of P(0/1) and P(1/0) as

$$P(0/1) = \frac{1}{\sigma_1\sqrt{2\pi}} \int_{-\infty}^{I_d} \exp\left(-\frac{(I-I_1)^2}{2\sigma_1^2}\right) dI \tag{3.31}$$

$$P(1/0) = \frac{1}{\sigma_0\sqrt{2\pi}} \int_{I_D}^{\infty} \exp\left(-\frac{(I-I_0)^2}{2\sigma_0^2}\right) dI \tag{3.32}$$

where σ_1^2 and σ_0^2 are the corresponding noise variances. From the definition of the complimentary error function we have

$$erfc(x) = \frac{2}{\sqrt{\pi}} \int_{x}^{\infty} \exp(-x^2) dx \tag{3.33}$$

using eq. (3.32.) in eq.(3.30) and (3.31) we get

$$P(0/1) = \frac{1}{2} erfc\left(-\frac{(I_1 - I_D)}{\sqrt{2}\sigma_1}\right) \tag{3.34}$$

$$P(1/0) = \frac{1}{2} erfc\left(-\frac{(I_D - I_0)}{\sqrt{2}\sigma_0}\right) \tag{3.35}$$

using eqs. (3.33) and (3.34) in eq. (3.29) we can write the BER as

$$BER = \frac{1}{4}\left[erfc(\frac{(I_1 - I_D)}{\sqrt{2}\sigma_1}) + erfc(\frac{(I_D - I_0)}{\sqrt{2}\sigma_0})\right] \tag{3.36}$$

eq (3.35) shows that the BER depends on the decision threshold I_D.

The required SNR to maintain particular bit error rates may be obtained using procedure adopted for error performance of electrical digital systems where the noise distribution is considered to be white Gaussian. This Gaussian approximation is sufficiently accurate for design purposes and is far easier to evaluate than the more exact probability distribution within the receiver.

Two types of noises, such as, thermal noise and shot noise are considered and also assumed that all these noises have Gaussian distribution. It is assumed that lights from all optical sources have an identical state of polarization, which corresponds to considering the worst case situation for system degradation. We also consider the XPM in the BER performance analysis.

3.5 Thermal noise

Thermal noise is the spontaneous fluctuation due to thermal interaction between, say, the free electrons and the vibrating ions in a conducting medium, and it is especially prevalent in resistors at room temperature. The thermal noise current is mean square value is given below.

$$P_{th} = \text{Thermal noise} = 4kTB/R_L \tag{3.37}$$

Where ,

k= Boltzmann's constant, T= Absolute temperature and B = Post detection bandwidth of the system

3.6 Shot noise

Shot noise occurs due to radiation. In fiber optic communication system, due to background radiation, some electron or charge penetrate rapidly and generate noise. The noise in mean square value is given below.

$$P_{shot} = \text{Shot noise} = 2eI_sB \tag{3.38}$$

Where,

E= Charge on an electron

I_s = Current

B= Post detection bandwidth of the system.

3.7 Expression of BER with XPM

The probability of error or bit Error rate (BER) is given by

$$BER(P_e) = 0.5erfc[SNR] \tag{3.39}$$

$$\text{where, } SNR(r) = \frac{I_s}{\sigma\sqrt{2}} \tag{3.40}$$

$$\text{where } I_s = R_d P_s(r) \tag{3.41}$$

$$\text{and } \sigma = \sqrt{P_{th} + P_{shot} + P_{XPM}} \tag{3.42}$$

where $P_{th} = \frac{4kTB}{R_L}$

and, $P_{shot} = 2eI_sB$

where B=Bandwidth, e= Electron charge

and $P_{XPM} = \Delta P_{jk}(\Omega, L_N)$ = Normalized XPM power transfer function

3.8 Simulation setup and description

Rsoft's OptSim simulation software is used to simulate the XPM crosstalk performance in presence of chromatic dispersion. OptSim gives us the environment almost the exact physical realization of a system. It provides the users with laser diodes, filters, modulators and all the components which are essential to build an optical network. The simulation setup for 2-channel and 4-channel for a NRZ modulated WDM system is shown in Fig. 3.3 and Fig. 3.4 respectively.

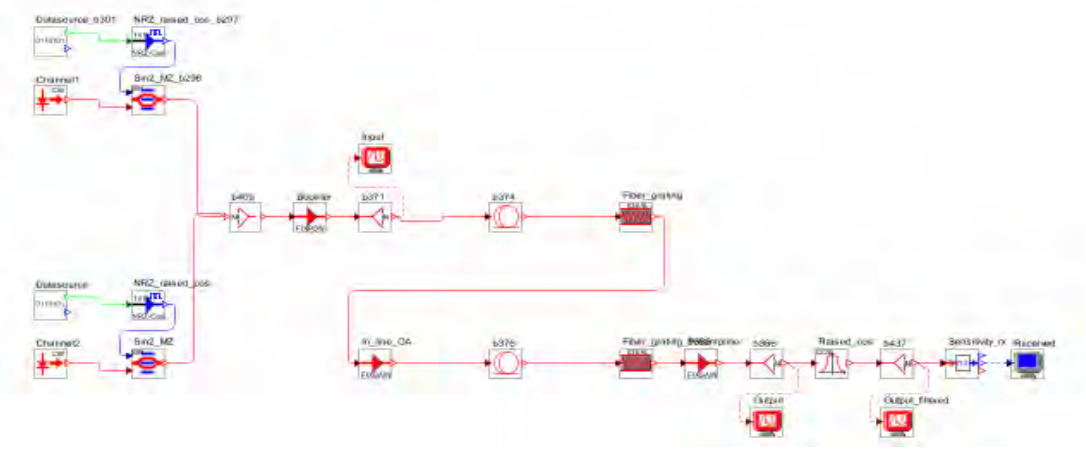

Fig. 3.3: Setup of the system simulation model for 2-channel WDM/ IM-DD transmission system using DSF

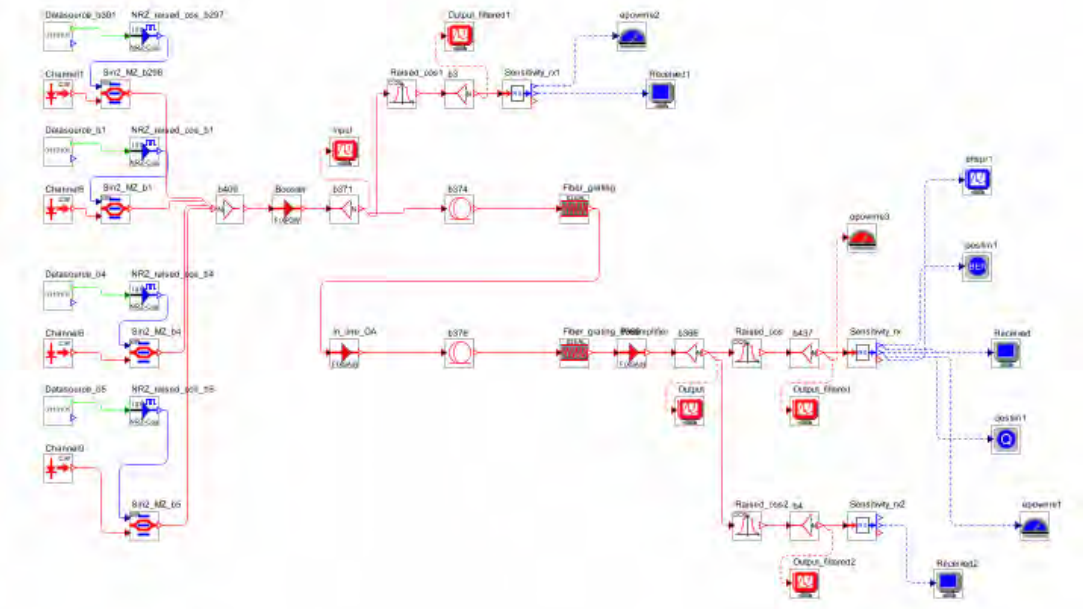

Fig. 3.4: Setup of the system simulation model for 4-channel WDM/ IM-DD transmission system using DSF

This simulation is carried out in presence of CD. In Fig.3.3 and Fig. 3.4 2-WDM channel and 4- WDM channel (bit rate 10 Gbps/channel) are launched over two DSF (2- span of 100 km each) respectively . Here the fiber loss is totally compensated by the EDFA and CD is completely compensated at each span by the fiber Bragg grating. The interaction of XPM depends upon the fiber's CD due to walk off effects between the pump and probe. So, we varied the CD from 0 - 6 ps/nm-km and observe XPM effects on the transmission system. This system consists of transmitter section, fiber section and receiver section.

3.8.1 Transmitter section

The transmitter consists of the pseudo random bit sequence (PRBS) generator, which generates bit rate at 10 Gb/s with 2^7 –1 bits. This bit sequence is fed to the NRZ coder that produces an electrical NRZ coded signal. Two channels are used in this simulation. The pumps signal which have higher power and which produce phase modulation of the neighboring channel. The modulator used here is the Mach-Zehnder modulator. It has two inputs, one for the laser diode and the other for the data from the channels. There are two Mach-Zehnder modulators used, one for pump channel and one for probe channel. It converts the electrical signal into optical signal form.

3.8.2 Fiber section

The waveform is fed into the fiber which is a standard single mode fiber. This is a simplified version of the universal fiber module for simulation of wideband nonlinear signal transmission in optical fibers. The fiber model in OptSim takes into account the unidirectional signal flow, Kerr nonlinearity and dispersion. In our case, we take the dispersion shifted single mode fiber. We have set the length, dispersion parameters, attenuation, nonlinear index, core area of the fiber and XPM options. The parameters are adjusted according to the simulation. At the output of the fiber, the probe signal underwent XPM effect and the waveform at the output becomes distorted.

3.8.3 Receiver section

At the output of the trapezoidal filter, a photodiode converts the optical signal into an electrical signal. An electrical low pass Bessel filter follows the avalanche photodiode (APD). This has a cut-off frequency determined by the type of the waveform used for modulation. Finally at the output of the low pass filter, OptSim

provides a visualization tool called *Scope*. It is an optical or electrical oscilloscope with numerous data processing options, eye display and BER estimation features. If the eye opening is very wide and there is no crosstalk. An eye diagram is usually used to effectively analyze the performance of an optical system. Eye diagrams clearly depict the data handling capacity of a system. The more the eye is open, the more efficient the system. Performance degradation will directly affect the eye diagrams which in turn results in reduced eye opening and time jitter at the edges.

CHAPTER 4

Results and Discussion

4.1 Introduction

To verify the derived theoretical expressions developed in the earlier chapters, numerical solutions have been achieved by means of Matlab to produce graphical results by varying different parameters. Here we have used 3- types of fibers, such as- SSMF, DSF and LEAF, and compared their XPM induced crosstalk performance. Though the analytical model is developed for multi-channel and multi-span system, most results are depicted for pump-probe configuration. We have also carried out simulation to find the impact of XPM for DSF fiber only using OptSim simulation software. Different system parameters of 3- types of fiber are shown in Table 4.1.

Table 4.1: Different system parameters

Parameter (unit)	**SSMF**	**DSF**	**LEAF**
Probe wavelength (nm)	1559	1559	1559
Channel spacing (nm)	0.4, 0.8, 1.6	0.4, 0.8, 1.6	0.4, 0.8, 1.6
Zero dispersion slope ($ps/nm^2/nm$)	0.095	0.075	0.084
Effective Area (m^2)	$8.0X10^{-11}$	$5.5X10^{-11}$	$7.2X10^{-11}$
Attenuation parameter (dB/km)	0.25	0.25	0.25
Dispersion Parameter (ps/nm/km)	17	3.5	4.5
First order GVD (ps^2/nm)	0.206	0.4515	0.3349
Second order GVD(ps^3/nm)	0.192295	0.1995	0.1957
Span Length (km)	100	100	100
Input pump power (dBm)	11.5	11.5	11.5
Input Probe Power (dBm)	11.5	11.5	11.5

4.2 Crosstalk in presence of GVD using SSMF

Using the developed analytical model, amount of normalized cross talk is calculated using SSMF for three different channel spacing. We have observed the variation of XPM crosstalk in presence of first- and second order GVD. Fig.4.1 shows the plots of normalized crosstalk vs. modulation frequency for various channel spacing in presence

of first order GVD. Fig. 4.2 shows the effect of crosstalk due to combined presence of first- and second order GVD and Fig. 4.3 presents crosstalk vs. modulation frequency with only second order GVD. It is found that the spectral characteristics of the fiber depend on the channel spacing and as a result at higher modulation frequency and lower channel spacing the amount of crosstalk increases. For example, at 10 GHz modulation frequency and 0.8 nm and 1.6 nm channel spacing the crosstalk is -54 dB and -58 dB respectively. It is also observed that at very lower modulation frequency (≤2 GHz) the crosstalk is very negligible.

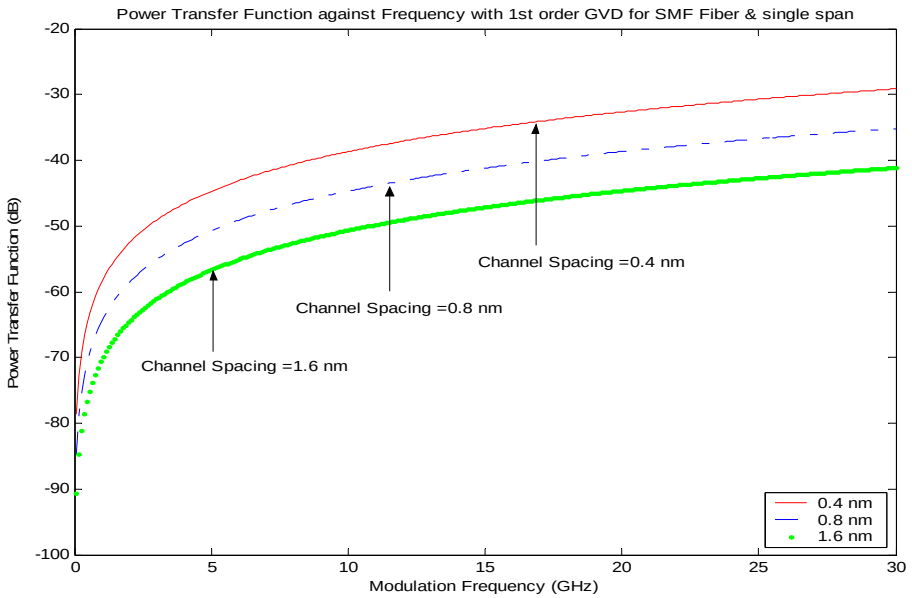

Fig. 4.1: Plots of crosstalk vs. modulation frequency with first order GVD for single span using SSMF

It is also observed that there is no appreciable difference between the plots of Fig. 4.1 and of Fig. 4.2. Actually, in presence of first order GVD, the second order GVD has negligible XPM crosstalk impact.

From Fig. 4.3, it is found that at 10 GHz modulation frequency and 0.8 nm channels spacing, the crosstalk is about -100 dB. Through, in absence of first order GVD this amount is quite low, but for a long-haul and high bit rate first order GVD compensated optical transmission system, the second order GVD become significant and limits the system performance.

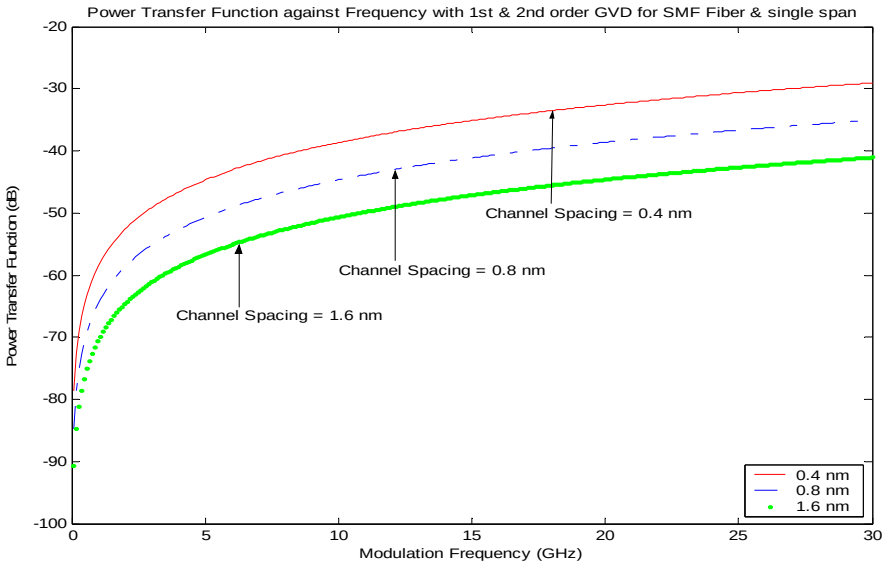

Fig. 4.2: Plots of crosstalk vs. modulation frequency with first and second order GVD for single span using SSMF

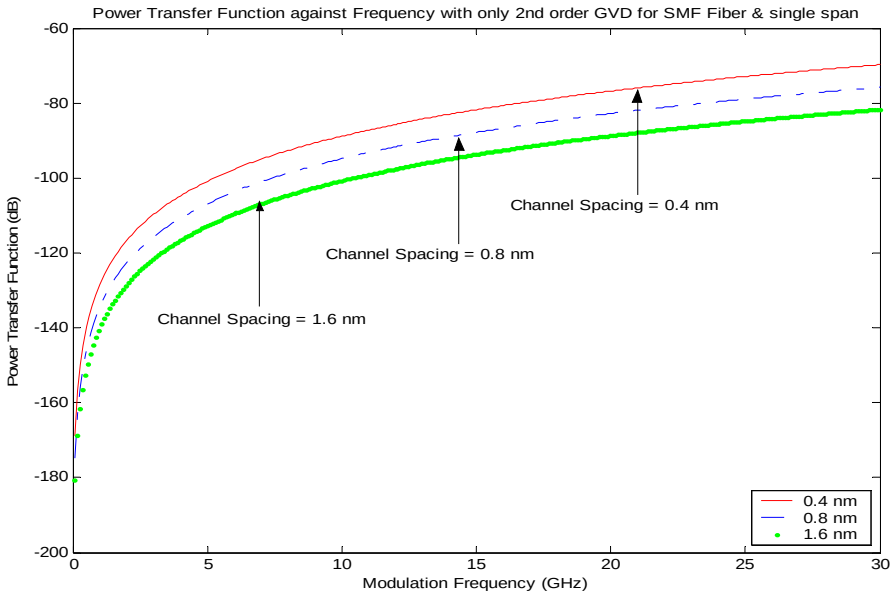

Fig. 4.3: Plots of crosstalk vs. modulation frequency with second order GVD for single span using SSMF

4.3 Crosstalk in presence of GVD using DSF

Fig. 4.4 and Fig. 4.5 are plots of crosstalk in presence of first order- and combined GVD respectively. Fig. 4.6 shows the impact of second order GVD on XPM crosstalk only. All of these plots are similar to SSMF, but amount of crosstalk is different. For instance (from Fig. 4.4 and Fig. 4.5), at 10 GHz modulation frequency and

0.8 nm channel spacing the amount of crosstalk are -25 dB and -24 dB for first order- and combined GVD respectively. So, the effect of XPM is more in DSF than SSMF. Again, while considering the second order GVD alone (Fig. 4.6), the amount of crosstalk (for same modulation frequency and channel spacing) is -80 dB only.

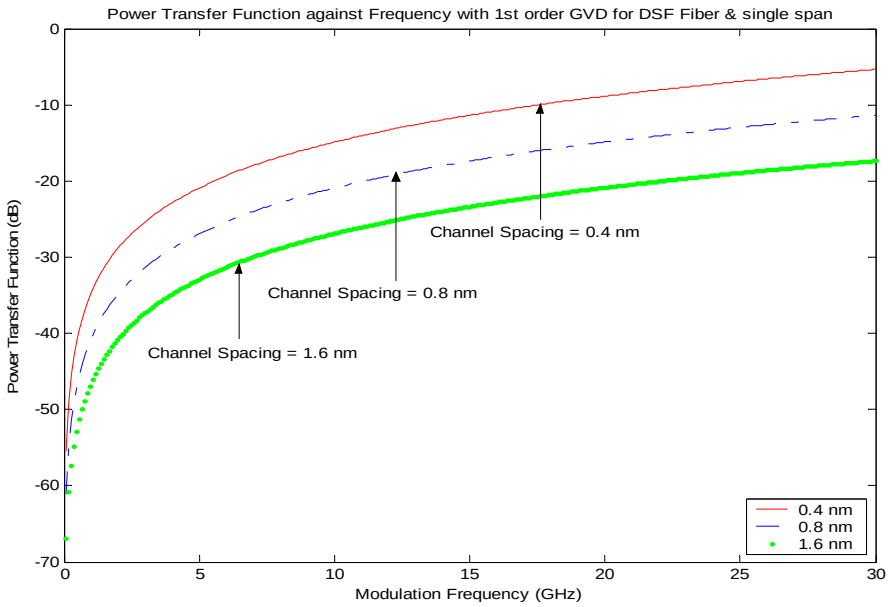

Fig. 4.4: Plots of crosstalk vs. modulation frequency with First order GVD for single span using DSF

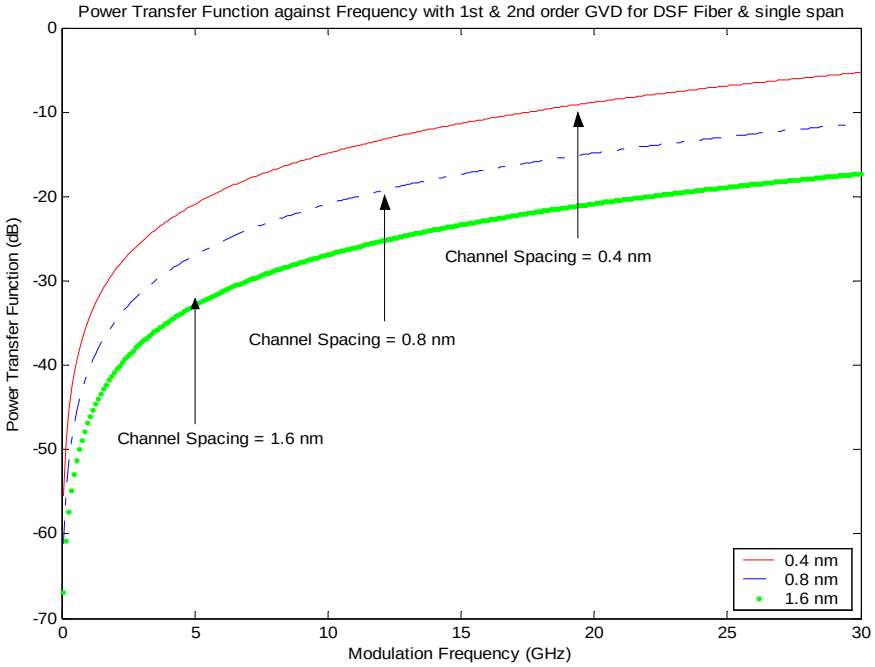

Fig. 4.5: Plots of crosstalk vs. modulation frequency with first and second order GVD for single span using DSF

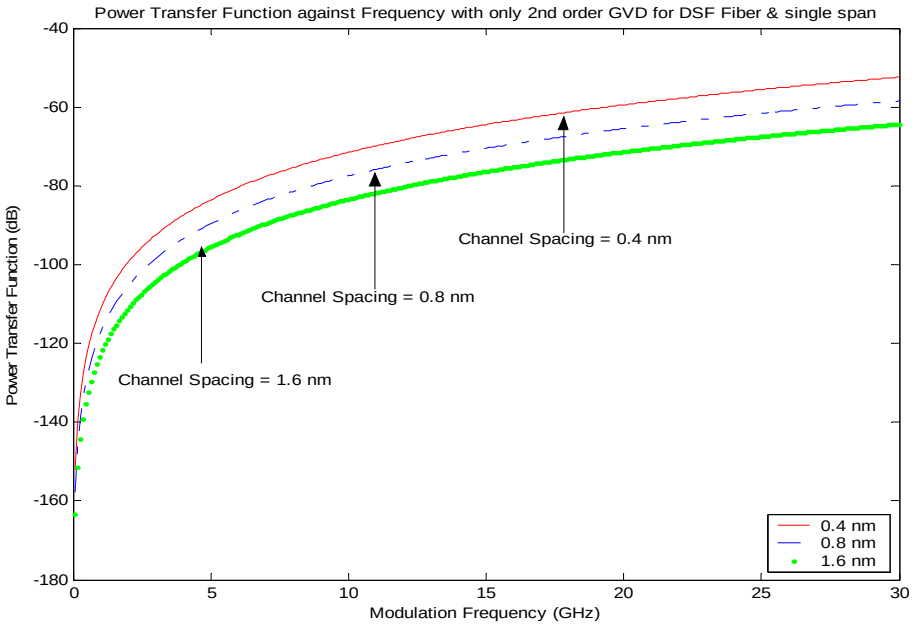

Fig. 4.6: Plots of crosstalk vs. modulation frequency with only second order GVD for single span using DSF

4.4 Crosstalk in presence of GVD using LEAF

LEAF fiber is developed by Corning Corporation Inc., USA to carry more optical power but with lower power density, alone inside core of the fiber. It operates in the wavelength 1550 nm -1575 nm ranges.

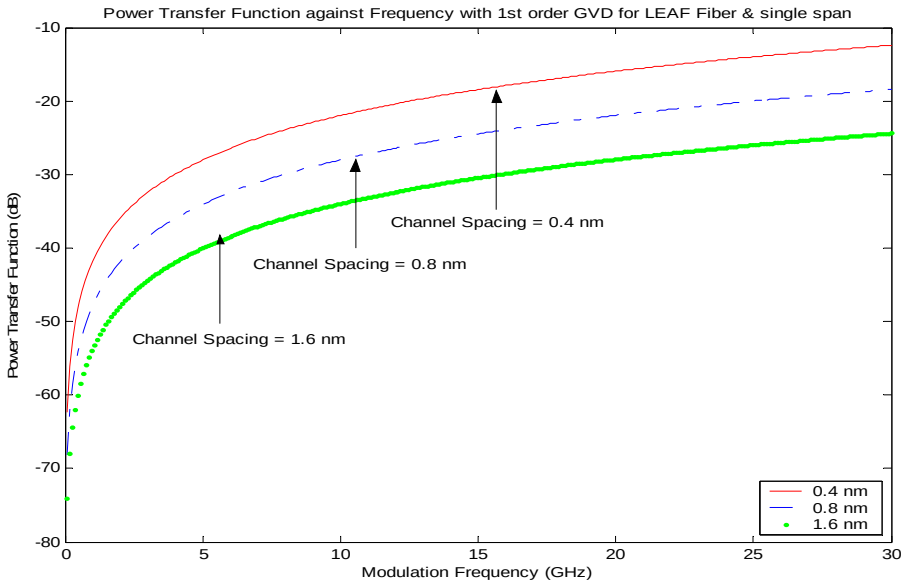

Fig. 4.7: Plots of crosstalk vs. modulation frequency with first order GVD for single span using LEAF

The effect of XPM crosstalk due to the presence of first order GVD, combined GVD and second order GVD only are depicted in Fig. 4.7, Fig. 4.8 and Fig. 4.9 respectively. From the plots it is observed that the effect of crosstalk in LEAF is less than DSF. For instance, at 10 GHz modulation frequency and 0.8 nm channel spacing the crosstalk is 2 dB less in LEAF than DSF in presence of first order GVD.

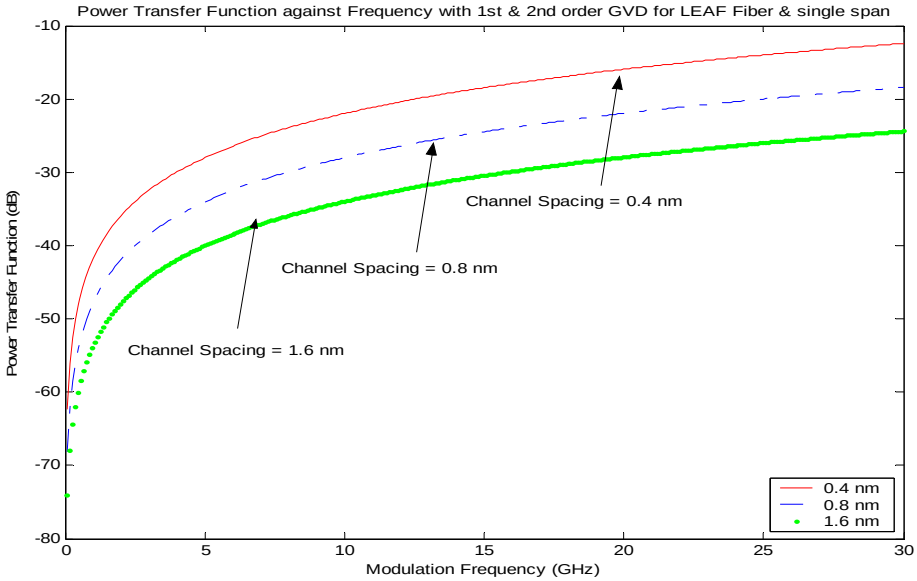

Fig. 4.8: Plots of crosstalk vs. modulation frequency with first and second order GVD for single span using LEAF

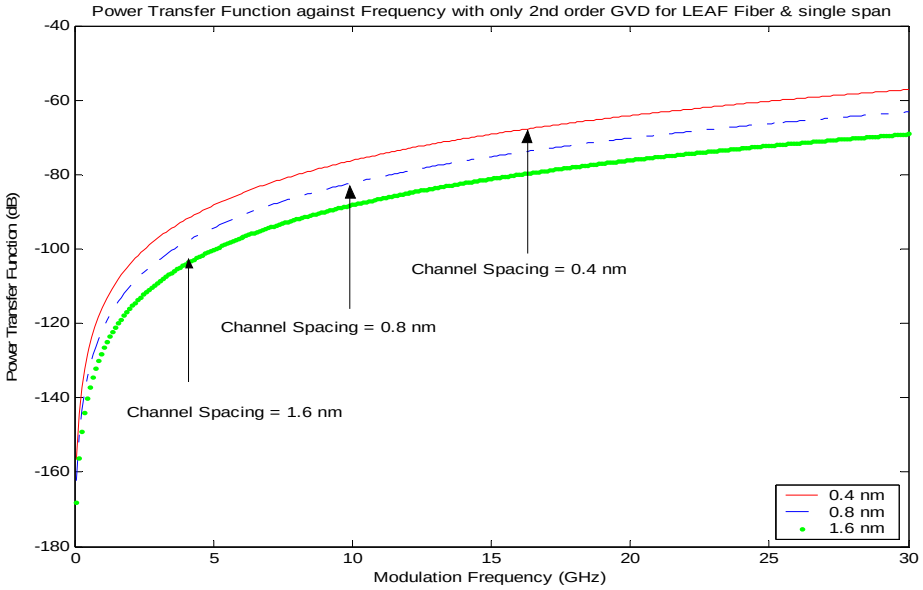

Fig. 4.9: Plots of crosstalk vs. modulation frequency with only second order GVD for single span using LEAF

4.5 Crosstalk in DSF for multi-span system

In the previous sections, all the results are obtained for single span system with span length of 100 km. We have derived crosstalk expression for multi-channel multi-span system. In this section, the XPM effect in a multi-span optical WDM system is observed. Fig. 4.10, Fig. 4.11 and Fig. 4.12 show the effects of XPM (three different channel spacing) in presence of first order GVD, combined GVD and second order GVD respectively.

From the plots, we have noted that the shape of XPM frequency response is dependent on the channel spacing. In the previous sections (for single span system), no ripples are observed plots (XPM induced crosstalk vs. modulation frequency), but for two span systems we found ripples. These ripples in the XPM spectrum are due to interference between XPM-induced crosstalk which is created in previous fiber span. It can be shown from equation (3.27) that the notches in the spectrum are located at frequencies which satisfy approximately the relation,

$$1+e^{i\Omega d_{jk}L_1}=0 \qquad (4.1)$$

and, therefore, the frequency difference between adjacent notches of a spectrum is $\Delta f = 1/(d_{jk}L_1)$, where L_1 is the fiber length of the first span.

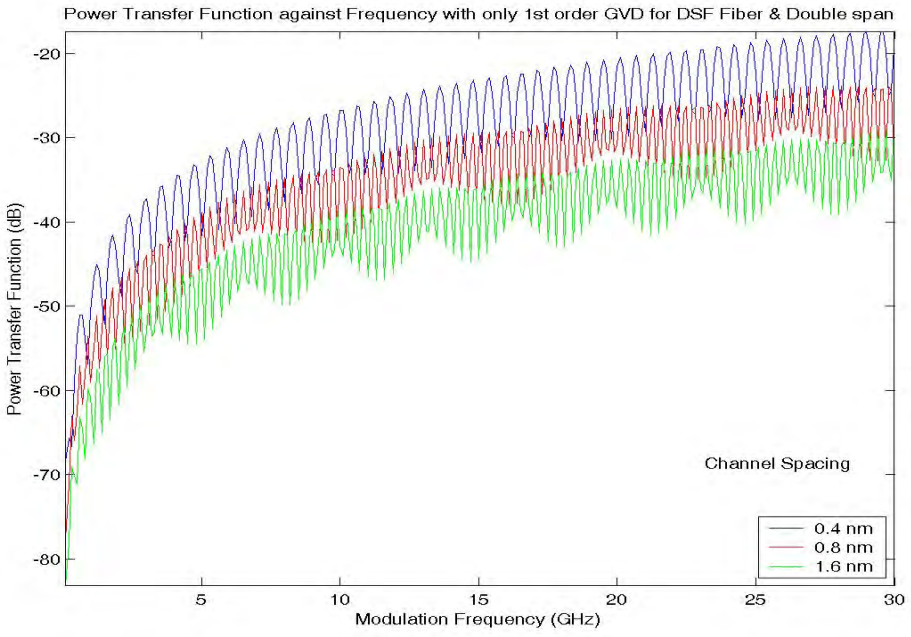

Fig. 4.10: Plots of crosstalk vs. modulation frequency with first order GVD for two span using DSF

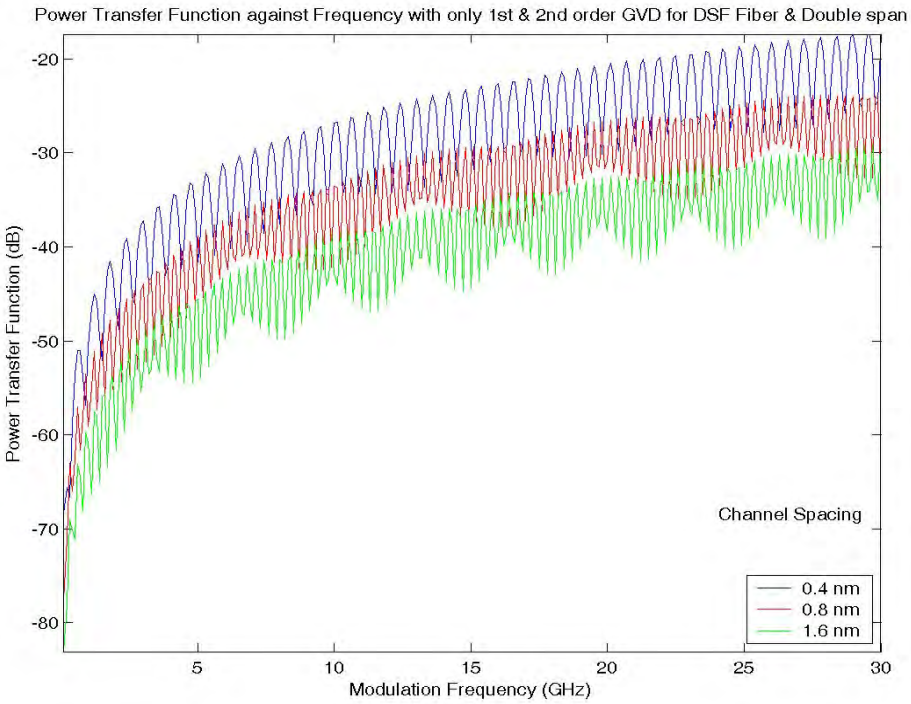

Fig. 4.11: Plots of crosstalk vs. modulation frequency with first and second order GVD for two span using DSF

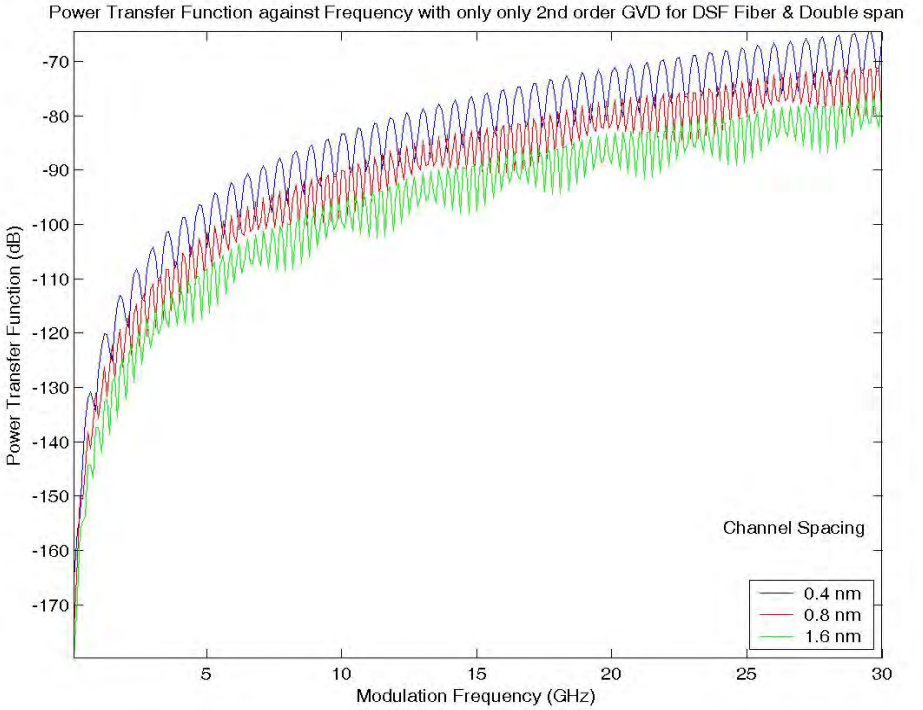

Fig. 4.12 plots of crosstalk vs. modulation frequency with only second order GVD for two span using DSF

4.6 Effect of channel number on XPM crosstalk

Till now, we have discussed the crosstalk performance and its limitation due to XPM for pump-probe configuration with different span length and channel spacing using 3-types of fiber. In this section, we see the effect of channel number on XPM crosstalk. Fig. 4.13, Fig. 4.14 and Fig. 4.15 show the impact of XPM crosstalk vs. channel number for SSMF, DSF and LEAF respectively. From the results, it is found that as the channel number increases XPM crosstalk also increases for a fixed channel spacing & modulation frequency. For example, from Fig. 4.13 shows that in SSMF (channel spacing 0.8 nm and modulation frequency: 5 MHz) amount of crosstalk is -53 dB and -62 dB for 8 channels and 2 channels respectively. On the other hand, from Fig. 4.14, it is found that in DSF the crosstalk is -32 dB and -45 dB for 8 channels and 2-channels respectively for the same channel spacing and modulation frequency. So, we can conclude that crosstalk is directly proportional to the number of channels. The effect of crosstalk is found minimum in SSMF than DSF or LEAF for a fixed number of channels and at a particular modulation frequency.

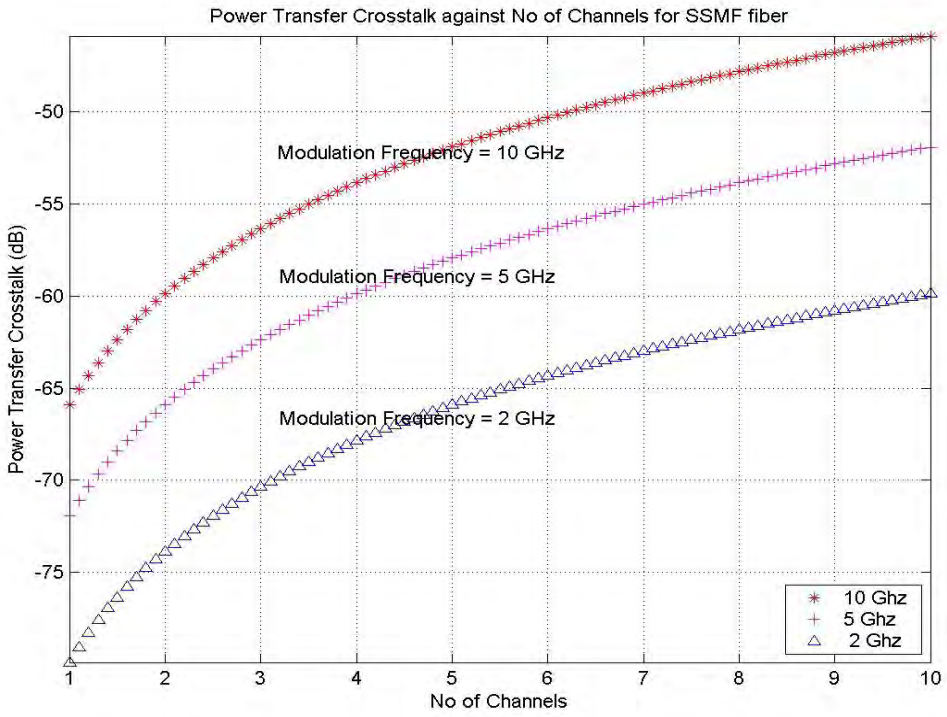

Fig. 4.13: Plots of crosstalk vs. number of channel for SSMF Fiber with various modulation frequencies

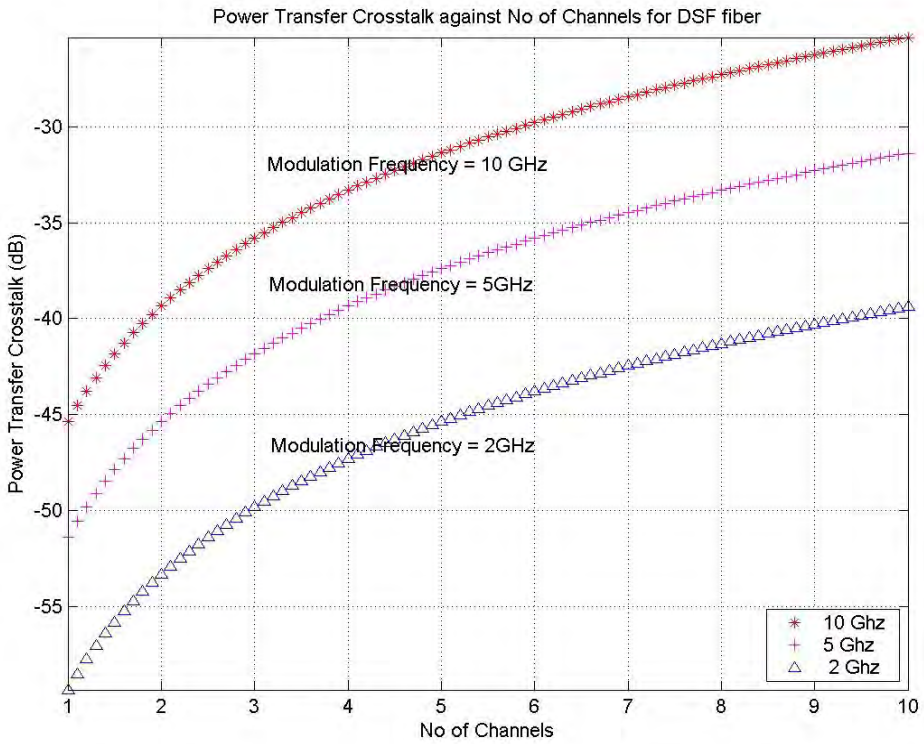

Fig. 4.14: Plots of crosstalk power vs. number of channel for DSF Fiber with various modulation frequencies

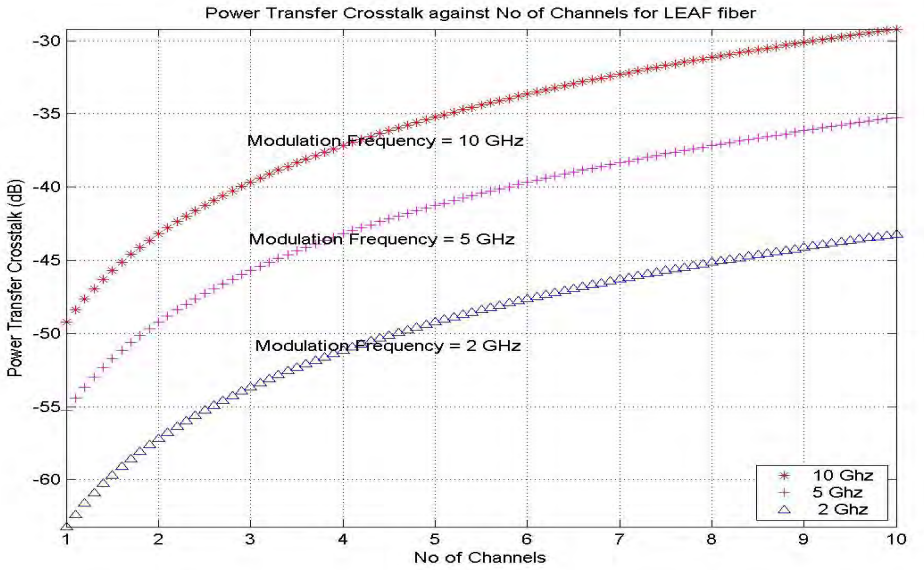

Fig. 4.15: Plots of crosstalk vs. number of channel for LEAF Fiber with various modulation frequencies

4.7 Effect of modulation frequency on XPM crosstalk

In section 4.2, section 4.3 and section 4.4, we have studied the effect of XPM crosstalk on modulation frequency by varying the channel spacing for 3-types of fiber and found

that at narrow channel spacing crosstalk is higher. In this section, we have tried to observe the effect of crosstalk on channel number for a fixed modulation frequency. Fig. 4.16, Fig. 4.17 and Fig. 4.18 are plotted for crosstalk noise for SSMF, DSF and LEAF. Results show that as the number of channel increases the XPM crosstalk also increases.

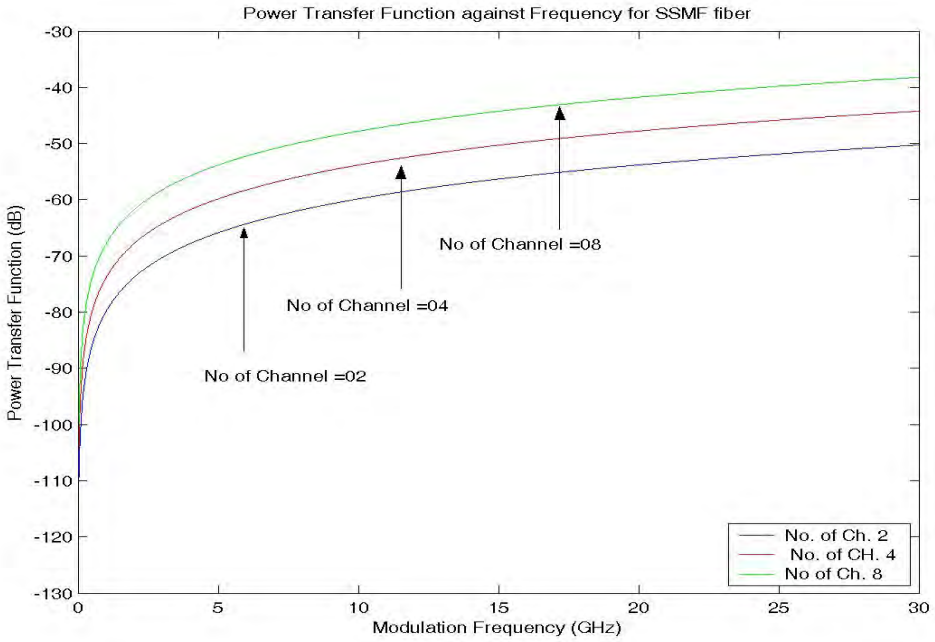

Fig. 4.16: Plots of crosstalk vs. modulation frequencies for SSMF with various no of channel

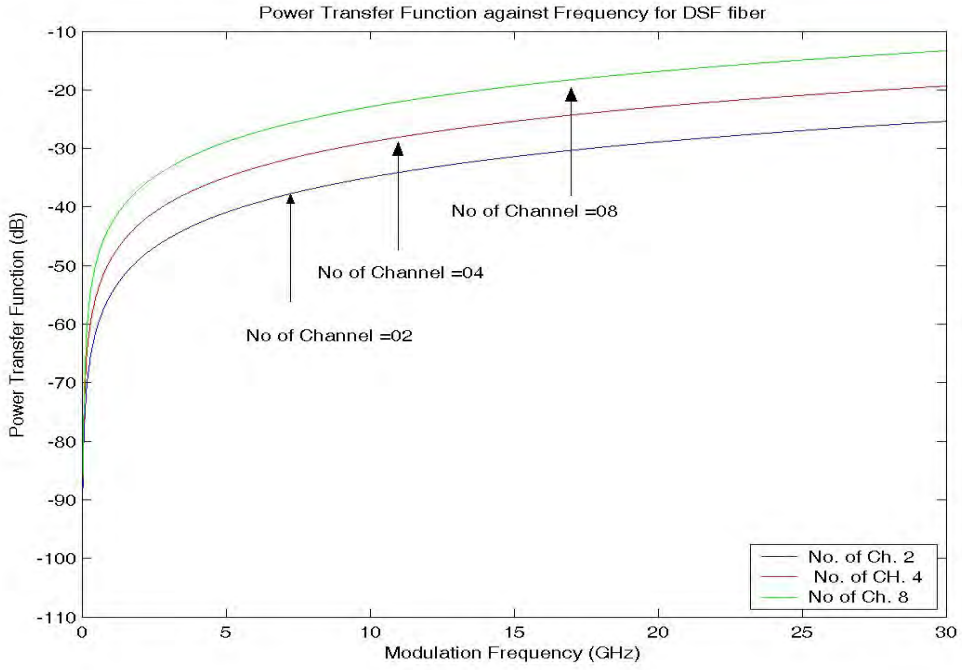

Fig. 4.17: Plots of crosstalk vs. modulation frequencies for DSF with various no of channel

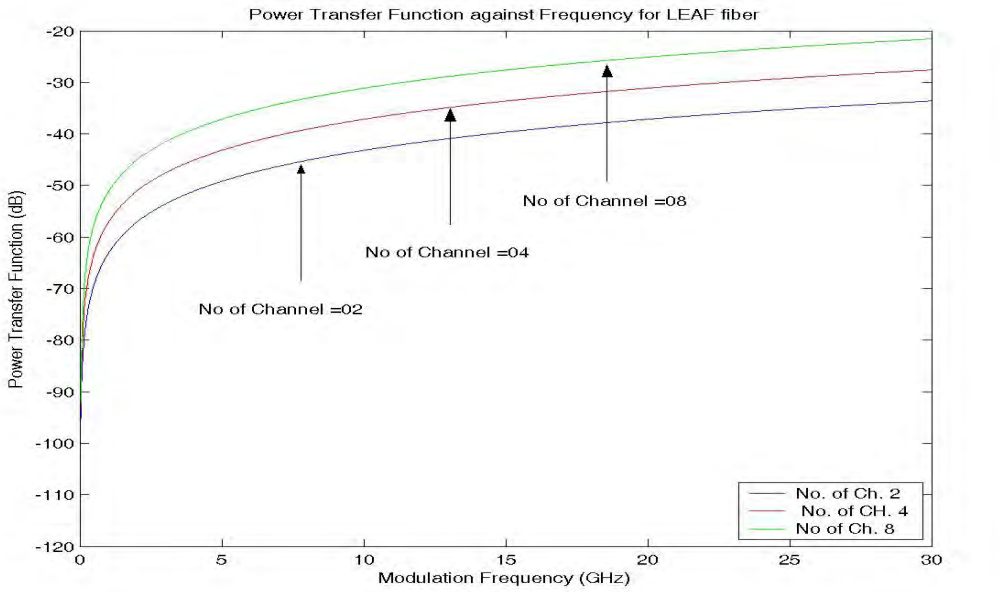

Fig. 4.18: Plots of crosstalk vs. modulation frequencies for LEAF with various no of channel

4.8 Comparison among SSMF, DSF and LEAF in presence of first order GVD

To compare the amount of crosstalk among SSMF, DSF and LEAF, we have plotted crosstalk versus modulation frequency in presence of first order GVD in Fig. 4.19. The results show that XPM crosstalk penalty due to first- order GVD is 23 dB and 7 dB more in DSF than that of SSMF and LEAF respectively at 10 GHz modulation frequency and 0.8nm channel spacing.

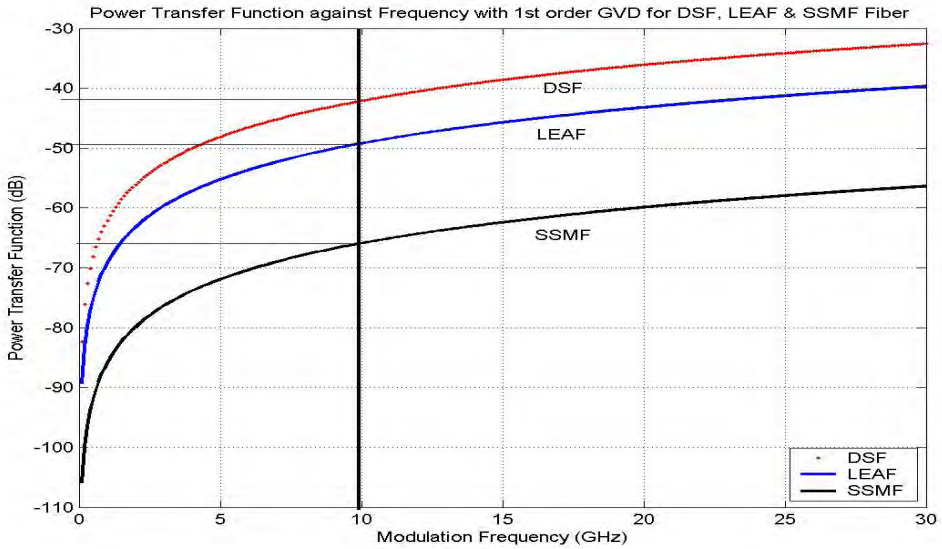

Fig. 4.19: Plots of crosstalk vs. modulation frequencies in presence of first GVD for various fibers

4.9 Comparison among SSMF, DSF and LEAF in presence of first order GVD

The plots of crosstalk versus modulation frequency in presence of second order GVD only are shown in Fig. 4.20 for 3-types of fiber. It is observed that XPM crosstalk penalty in DSF is 16 dB and 4 dB more in DSF than that of SSMF and LEAF respectively at 10 GHz modulation frequency and 0.8nm channel spacing.

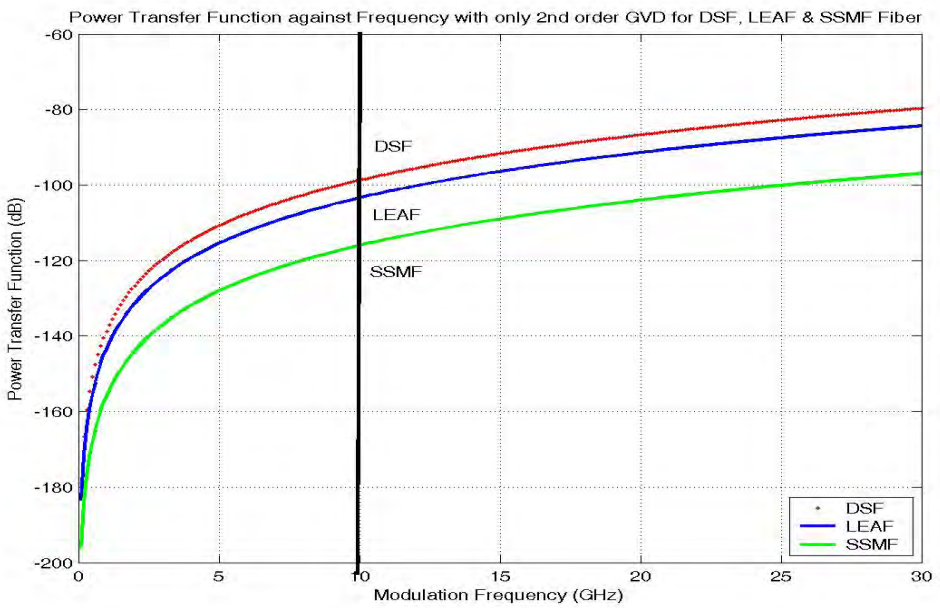

Fig. 4.20: Plots of crosstalk vs. modulation frequencies in presence of second order GVD for various fibers

4.10 Effect of second order GVD in long haul system

In Sections 4.2 (Fig. 4.3) , 4.3 (Fig. 4.6) and 4.4(Fig. 4.9), we have studied the effect of second order GVD on XPM (span length 100 km) in first order GVD compensated transmission system for SSME, DSF and LEAF respectively. We observed that the effect of second order GVD on the system performance is negligible. But in practical long haul WDM system, the effect of second order becomes significant. This is depicted in Fig. 4.21, where we have determined the effect of second order GVD only for 0.8 nm channel spacing for various span lengths of SSMF. From the figure it is found that at 10 GHz modulation frequency the crosstalk is -105 dB, -78 dB and -65 dB for fiber length of 100 km, 1000km and 10,000 km respectively. Thus, we can conclude that in long haul high bit rate WDM system second order GVD plays a crucial role in limiting the system performance.

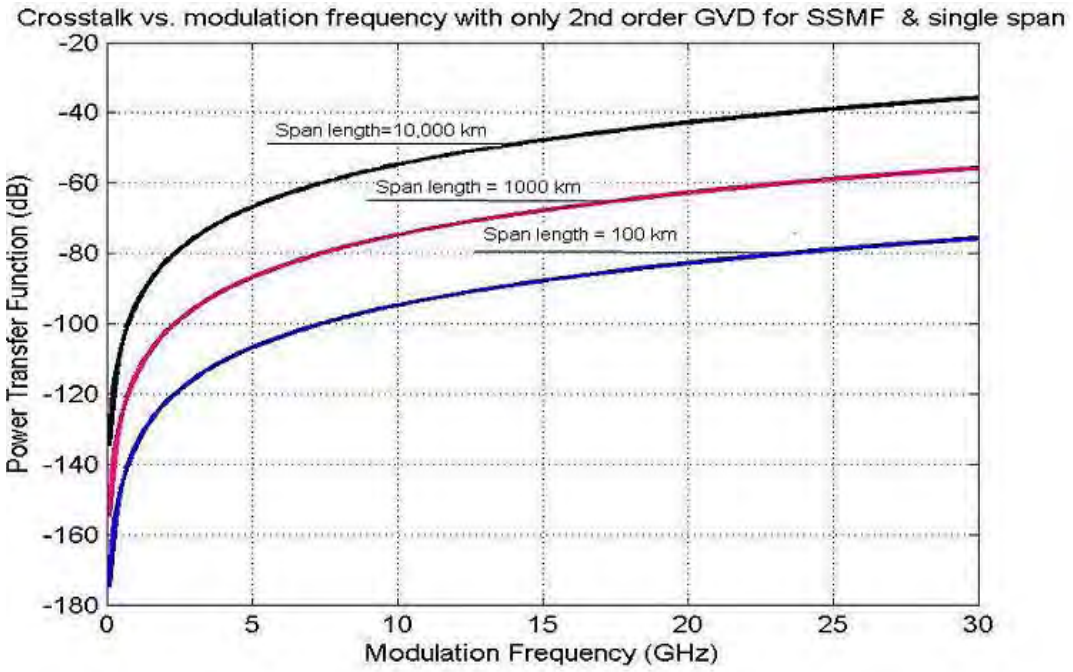

Fig 4.21: Crosstalk vs. modulation frequency for various span lengths in presence of second order GVD only

4.11 Comparison with the published results: single- and multi-span

The effect of crosstalk due to XPM only in presence of first order GVD is theoretically and experimentally is shown by Hue *et al.* [16] for DSF fiber. We have also derived normalized crosstalk incorporating first- and second order GVD.

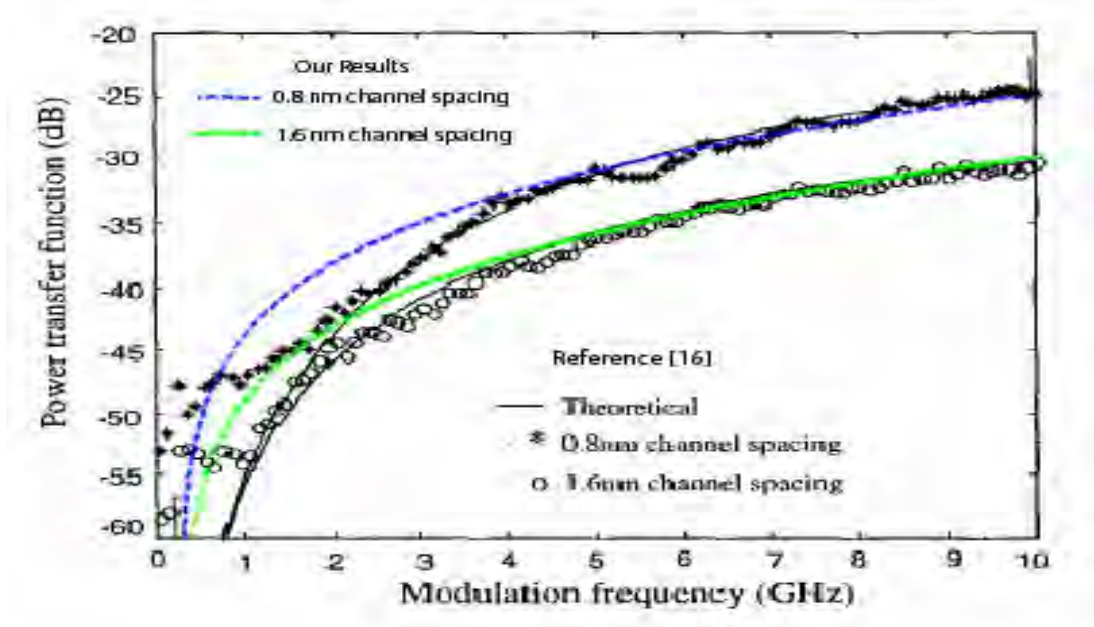

Fig. 4.22 : XPM frequency response in the system with single span (114 km) DSF fiber for 0.8 nm and 1.6 nm, λprobe = 1559 nm, n_2=2.35 X 10^{-20} m^2/W, A_{eff} = 5.5 X 10^{-11} m^2 and α=0.25 dB/km

We have put second order GVD, β_3=0 in equation (3.27) and the same parameters as in [16], we computed the results and compared with [16]. The combined curves are shown in Fig. 4.22. It is found that our computed results and the reference [16] graph are very much similar by value and pattern.

The plots crosstalk versus modulation frequency for 2-span system with 0.8 nm and 1.6 nm channel spacing using same fiber and same parameter are compared with the reference [16] graphical representation (Fig. 4.23). In [16], they have considered the first- and second span length 116 km and 114 km DSF respectively. It is observed for 1.6 channel spacing the pattern of the graph are very similar to [16], but the fluctuations of crosstalk value does not match exactly. The maxima and minima occur at different modulation frequencies. For 0.8 nm channel spacing case, the ripples are more than [16], but pattern follows the trend.

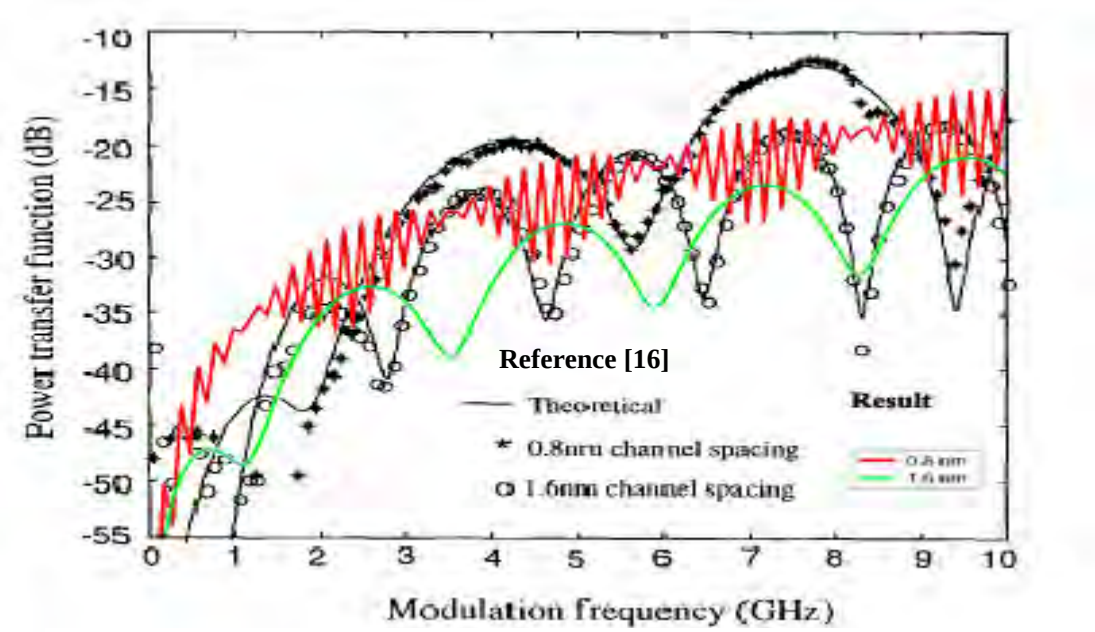

Fig. 4.23: XPM frequency response in the system with two span (114 km and 116 km) DSF fiber for 0.8 nm and 1.6 nm, λprobe = 1559 nm, n_2=2.35 X 10^{-20} m^2/W, A_{eff} = 5.5 X 10^{-11} m^2 and α=0.25 dB/km.

4.12 Simulation Results

In this thesis, we also investigate the effect of XPM on WDM optical transmission system in terms of eye diagram and BER in presence of GVD using Rsoft's OptSim simulation software for DSF. The channels are modulated at 10 Gbps data rate using

NRZ format and separated by 0.8 nm, the distance between the inline optical EDFA fiber amplifiers is 100 km (span length).

4.13 Pump and probe optical input/output spectrum

The input and output optical spectrum of the pump and probe is shown in Fig. 4.24 and Fig. 4.25 respectively. It is noticed that after propagating 100 km fiber link the optical due to the effect of fiber nonlinearity the output spectrum is distorted and two new frequencies are generated.

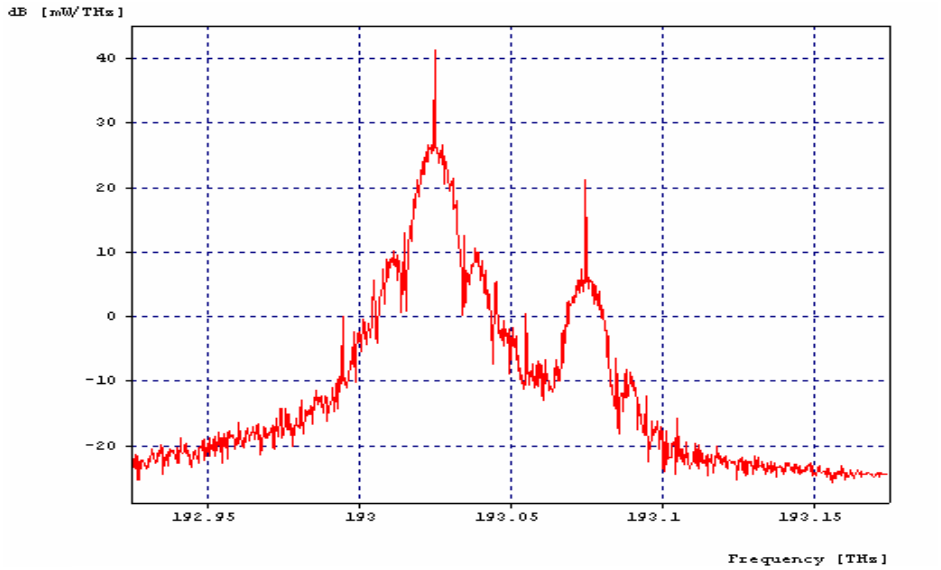

Fig. 4.24: Pump and probe optical spectrum at the input for 2-channel WDM system

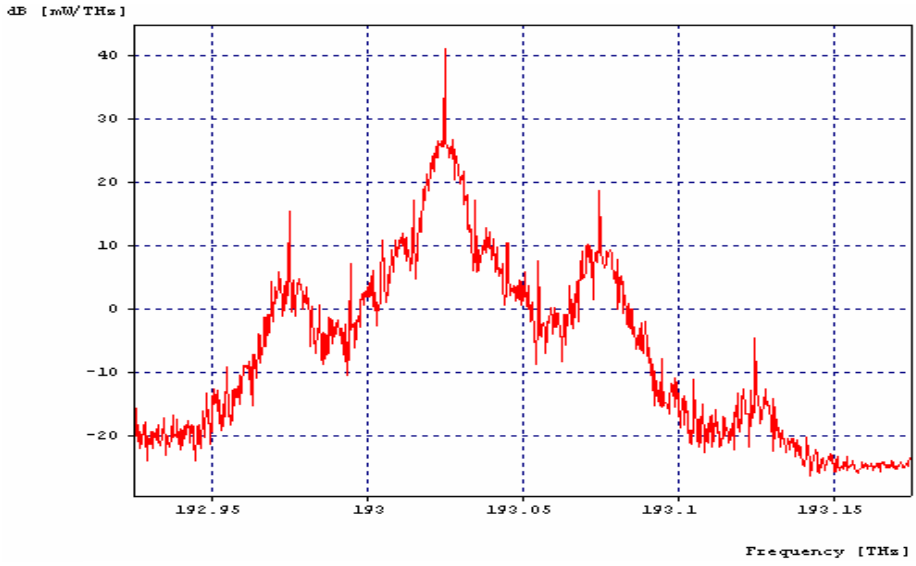

Fig. 4.25: Pump and probe optical spectrum at the output for 2-channel WDM system

4.14 Eye diagram of the probe

4.14.1 Two channel (pump-probe configuration) WDM system

To assess the impact of XPM on the transmission system in electrical domain, we first implement a 2-channel WDM system and monitor the probe signal eye diagram (by varying the dispersion coefficient) of the channels at the input (back-to-back) as well as at the output for a receiver sensitivity of -24 dBm (at a BER of 10^{-9}). Fig. 4.26 shows the eye diagrams at the input and output of the fiber link of different channels for different dispersion coefficient (0 - 4 ps/nm-km). We have observed that for a fixed channel spacing (50 GHz in this case or 0.8 nm) probe channel eye diagram deteriorates more at lower values of dispersion.

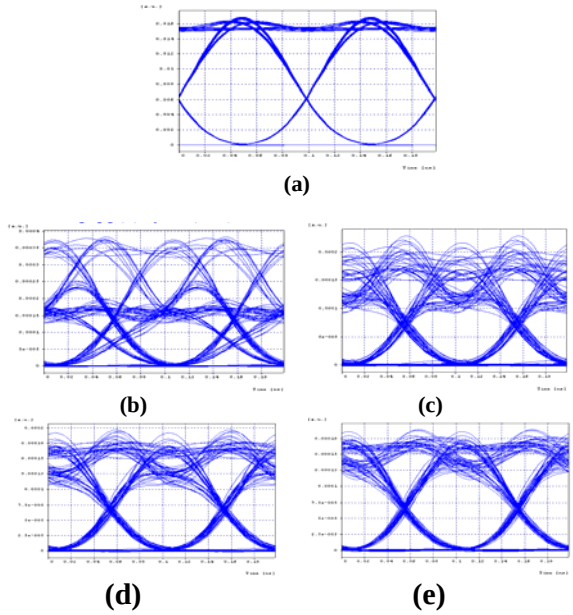

Fig. 4.26: (a) Base line eye diagram (back-to-back), (b) output eye diagram for D= 0 ps/nm-km (c) output eye diagram for D= 1 ps/nm-km (d) output eye diagram for D= 2 ps/nm-km and (e) output eye diagram for D= 4 ps/nm-km of probe signal.

4.14.2 4-channel WDM system

The 4-WDM channels are launched over two DSF fiber spans of 100 km each where fiber loss is totally compensated by the EDFA and CD is completely compensated at each span by the fiber Bragg grating. The interaction of CD with XPM due to walk off effects among the pumps and probe. So, we varied the CD from 1 - 2 ps/nm-km and observe its effect on the CD.

The channels are modulated at 10 Gbps data rate using NRZ format and separated by 0.8 nm, the distance between the inline optical EDFA fiber amplifiers is 100 km (span length). All the 4-incoming channels are multiplexed and transmitted through the fiber. At the receiving end, we demultiplexed the channels and monitor the signal on channel 2 (channel under study) and other channels. Fig.4.27 shows the eye diagram of the 4-channels at the input and output of the transmission system.

We found that the eye diagram channel under study (probe channel 2) is highly distorted at lower values of dispersion coefficient. From the simulation results (2-channel and 4-channel WDM) we found that XPM crosstalk effect is more at lower values of GVD.

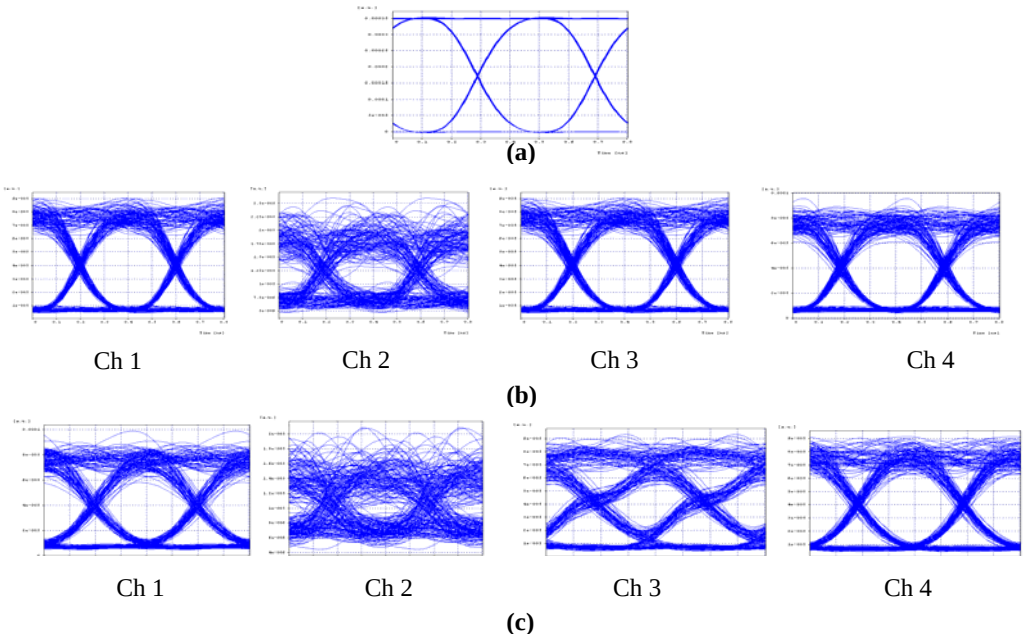

Fig. 4.27: (a) Base line eye diagram (back-to-back), (b) Channel 1- 4 at the output for a dispersion coefficient of 2 ps/nm-km; (c) Channel 1- 4 at the output for a dispersion coefficient of 1 ps/nm-km

4.15 Effect of pump and probe power variation

Plots of BER vs. input pump power and BER vs. input probe power are shown in Fig. 4.28 and Fig. 4.29 for various values of dispersion coefficient respectively. It is observed (Fig. 4.28) that the XPM impact is maximum at zero dispersion coefficient (*i.e.*, the BER is significantly higher, about 10^{-2}) and as the dispersion coefficient increases the effect is less due to the walk-off phenomenon. On the other hand, as

pumps power increases the BER also increases due to the larger effect of XPM on the probe signal. From Fig. 4.29, it is found that at zero dispersion the BER is irrespective of probe power. For other values of dispersion coefficient, increasing the input probe power has little impact on the BER performance.

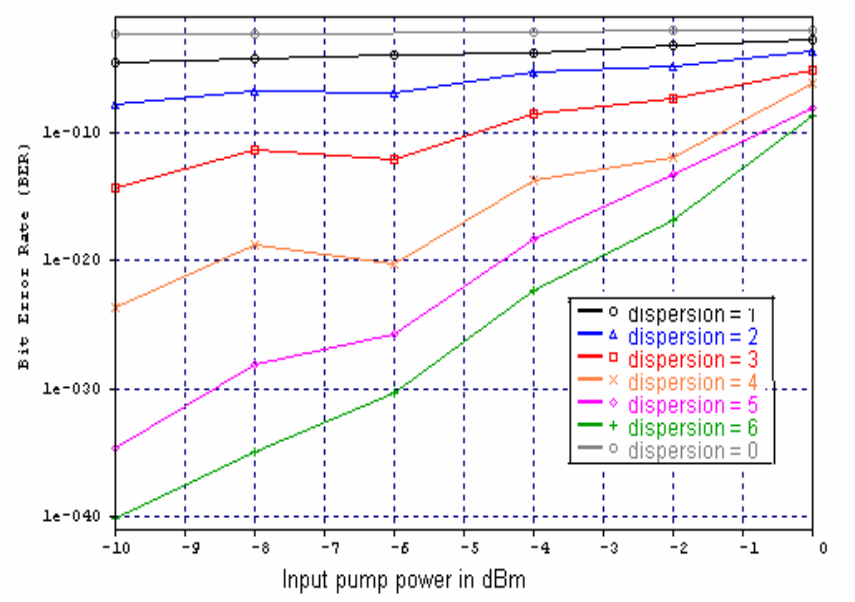

Fig. 4.28: BER vs pump power in dBm for different dispersion coefficient (probe power = - 30 dBm)

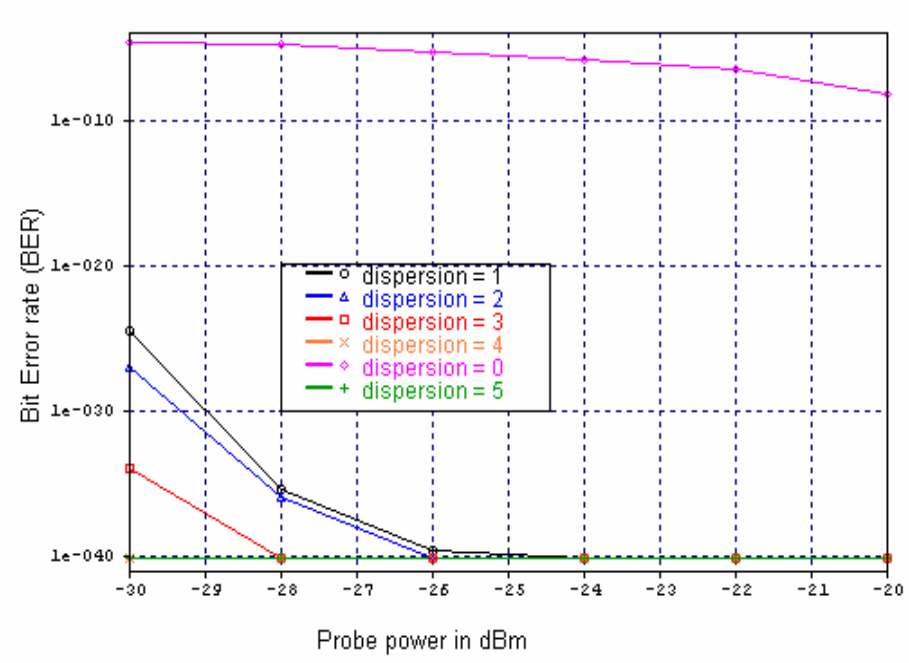

Fig. 4.29: BER vs. probe power in dBm for different chromatic dispersion coefficient (pump power= -10 dBm)

4.16 Eye opening penalty

We may calculate the average eye-opening penalty (EOP) due to XPM for the probe signal for 2-channel and 4-channel WDM system. Here, we define the parameter of the eye-opening penalty (EOP) as,

$$EOP = -20\log\left(\frac{B}{B_0}\right) \tag{4.2}$$

Where, B is the eye opening without XPM effect and B_0 is the eye-opening with XPM in the probe. From Fig. 4.30, it is observed that the EOP is highest at zero dispersion and becomes lower as the dispersion coefficient increases. For example, at dispersion 0.5 ps/nm-km the EOP is about 8.10 dB and at 4 ps/nm-km it is 1.45 dB in 2-channel WDM system. So, at higher dispersion the transmission is less affected by the XPM.

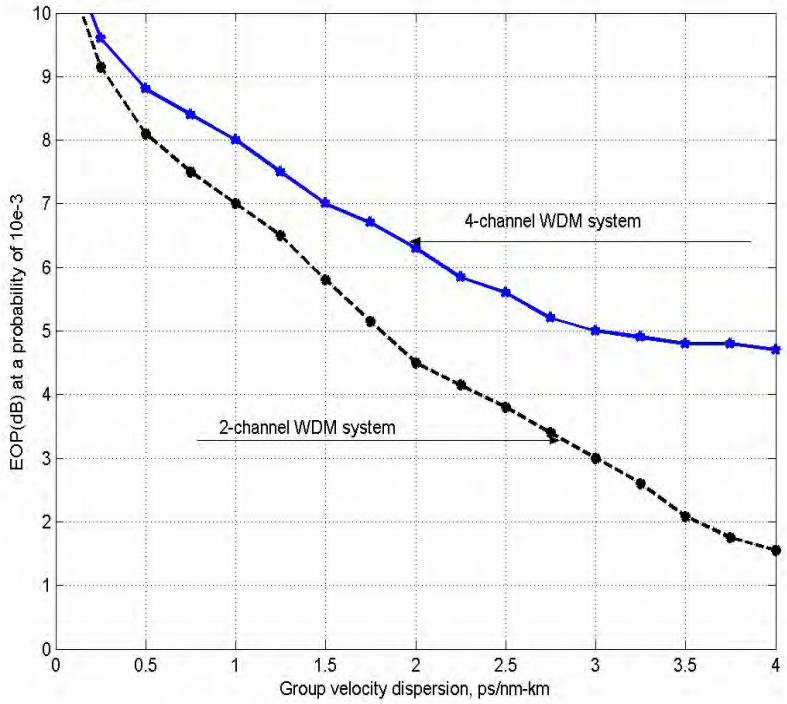

Fig. 4.30: Eye opening penalty (EOP) at a probability of 10^{-3} in the dependence of chromatic dispersion for 2-channel WDM transmission system

4.17 Discussion

A detailed computation and results analysis is carried out to evaluate the impact of XPM in WDM system in presence of first- and second order GVD. Results are evaluated and compared for commercially available SSMF, DSF and LEAF. We

observed that XPM has more impact on DSF fiber than that of SSMF and LEAF. It is also found that at shorten length the second order GVD has less impact on intensity fluctuation on the probe channel on WDM system, however at high bit rate if the first order GVD is zero then there is significant impact of second order GVD on optical transmission system. on the other hand when multi span system are consider then for long-haul transmission system second order GVD become prominent although first order GVD are compensated. We also observed that chromatic dispersion coefficient and group velocity dispersion are inter-related. It is also found that second order GVD is dependent on dispersion co-efficient as well as dispersion slope. As a result in first order GVD compensated system, dispersion slope of second order GVD play a critical role in limiting the performance in multi span WDM system.

CHAPTER 5

Conclusion and Future Work

5.1 Conclusion

The main motivation of this work is to study the effect of XPM in WDM optical transmission system in presence of first– and second order GVD. Fiber nonlinearities have become one of the most significant limiting factors of system performance. In WDM systems, inter-channel interference due to fiber nonlinearities limits the system performance significantly. Therefore, understanding of fiber nonlinearities is crucial to optimize system performance of optical fiber transmission. In this thesis, an analytical model is developed to evaluate the impact of XPM on high bit rate WDM optical systems.

The findings of this work are given below:

1. The crosstalk is strongly dependent on modulation frequency and channel spacing, *i.e*. at higher modulation frequency and narrow channel spacing the crosstalk effect becomes higher.

2. Out of the 3- types of fiber, the XPM effect is minimum in SSMF and maximum in DSF.

3. EOP is highest at zero dispersion and becomes lower at higher dispersion.

4. In multiple spans, XPM induced crosstalk creates ripples in the spectral response due to interference between crosstalk in the previous span.

5. XPM crosstalk increases with increasing number of channels for a constant modulation frequency.

6. In a first order GVD compensated system, the effects of second order GVD is negligible for single span system, but at high bit rate and large number of span this effect becomes significant and may limit the system performance greatly.

5.2 Recommendations for Future Work

Research work is a continuous process. So it is important to think about the scope of further extension of this work. We have analyzed a WDM system considering few channels at a time and data rate of 10 Gbps per channel. Further research may be carried out at data rate of 40 Gbps per channel and also accommodating large number (>16) of channels with various channel spacing even as small as 0.1 nm. It is also important to look into the methods and techniques for compensate the XPM impairment. Other nonlinear effects may be also considered to reflect the true performance limitations due to nonlinear phenomenon.

REFERENCES

[1] Basch, E. E., "Optical Fiber Transmission" First Edition, Academic Press, New York, 1986.

[2] Dang, N.T. and Pham, A.T., "Performance degradation of spectral amplitude encoding optical code division multiple access systems due to group velocity dispersion", Proc. of 14th Asia-Pacific Conference on Communication 2008 (APCC 2008), vol.1, pp. 1–5, 2008.

[3] Majumder, S. P., Islam, M. R. and Gangopadhyay, R., "Effect of group velocity dispersion on a WDM optical ring network", Proc. of Lasers and Electro-Optics Society Annual Meeting (LEOS '98), vol. 2, pp. 236 – 237, 1998.

[4] Agrawal, G. P, "Nonlinear Fiber Optics", San Diego, CA, Academic Press, 2001.

[5] Forghieri, F, Tkach, R. W. and Chraplyvy, A. R., "Fiber nonlinearities and their impact on transmission systems," in Optical Fiber Telecommunications IIIA, I. P. Kaminov and T. L. Koch, San Diego, CA, Academic, 1997.

[6] Karfaa, Y. M., Ismail, M., Abbou, F. M., Shaari, S. and Majumder, S. P. "Effects of cross-phase modulation crosstalk in WDM networks on received power and number of channels for various fiber types", Proc. of Asia Pacific Conference on Applied Electromagnetic (APCAE 2007), Malaysia, vol.1, pp. 22-27, 2007.

[7] Betti, S. and Giaconi, M., "Effect of cross phase modulation on WDM optical systems: Analysis of fiber propagation", IEEE Photonics Technology Letters, vol. 13, pp. 305-307, 2001.

[8] Kao, K.C. and Hockham, G.A., "Dielectric fiber surface waveguides for optical frequencies." Proc. of IEE, vol. 133, pp.1151-1158, 1966.

[9] Colas, T. M., Green, M., Wuzniak, G. and Arena, J., "The TAT-12/13 cable network" IEEE Communication Magazine, vol. 34, no.2, pp. 24-28, 1996.

[10] Barnett W.C., Takahira H., Baroni G. C. and Ogi., " The TPC-5 cable network.", IEEE Communication Magazine, vol.34, no.2, pp. 24-28, 1996.

[11] Sharif, M. and Alkhansari M. G., "On the peak to average power OFDM signals based on over sampling", IEEE Transactions on Communications, vol. 51, no. 1, pp. 72-78, 2004.

[12] Agrawal, G. P., "Fiber Optic Communication Systems", John Wiley and Sons, Singapore, 1993

[13] Arumugam, M., "Optical Fiber Communication —An overview", Pranama Journal of Physics, vol. 57, pp. 849–869, 2001.

[14] Hui, R., Wang, Y., Demarest, K., and Allen, C., "Frequency response of cross-phase modulation in multispan WDM optical fiber systems", IEEE Photonic Technology Letters, vol. 10, pp. 1271-1273.

[15] Majumder, S. P., Islam, M. R. and Gangopadhyay, R., "Effect of group velocity dispersion on a WDM optical ring network", Proc. of Lasers and Electro-Optics Society Annual Meeting (LEOS '98), vol. 2, pp. 236 – 237, 1998.

[16] Hui, R., Kenneth R., Demarest, and Christopher T. Allen, "Cross phase modulation in multispan WDM optical fiber systems", Journal of Lightwave Technology, vol. 17, no.6, 1999.

[17] Thiele H. J., Killey R.I. and Bayvel P.,"Pump-probe investigation of cross phase modulation in standard-fiber, dispersion compensated WDM recirculation loop", Conference on Lasers and Electro-optics, vol.1, pp. 305-306, 1999.

[18] Thiele H. J., Killey R.I. and Bayvel P., "Investigation of XPM distortion in transmission over installed fiber", IEEE Photonics Technology Letters, vol 12, no. 6, pp. 669-671, 2000.

[19] Hoon, K., "Cross phase modulation induced nonlinear phase noise in WDM direct detection DPSK systems", Journal of Lightwave Technology, vol. 21, no. 8, pp. 1126-1137, 2003.

[20] Goeger, G., Wrage, M., and Fischler, W., "Cross-phase modulation in multispan WDM systems with arbitrary modulation formats", IEEE Photonics Technology Letters, vol 16, no. 8, pp.1858-1860, 2004.

[21] Abdul-Rashid, H. A., Abbou, F. M., Chuah, H. T., Tayahi, M. B., Al-Qdah, M. T. and Lanka, S., "System performance optimization in SCM-WDM passive optical networks in the presence of XPM and GVD", IEEE Communications Letters, vol. 10, no. 9, 2006.

[22] Sakib, M. N., Alam, M. N, Sajjad, R. N, and Majumder S. P., "Impact of Cross-Phase Modulation on the Performance of a WDM Optical Transmission System with Short- Period Dispersion Managed Fiber", 3rd International Conference on Computers and Devices for Communications (CODEC-06), pp.525-527, 2006.

[23] Lee, M., and Neo Antoniades, "On the impact of filter dispersion slope on the performance of 40 Gbps DWDM systems and networks" Photon networking Communications, 2007.

[24] Rashid, H. A. A., Abbou, F.M., Al-Qdah, M.T., Chuah, H.T. and Tayahi, M.B., "Semi-analytical performance analysis of an SCM-WDM PON in the presence of XPM and GVD", IEEE International Conference on Telecommunications, Malaysia, pp.35-38, 2007.

[25] Karfaa, Y. M., Ismail, M., Abbou, F. M., Shaari, S. and Majumder, S. P., "Effects of cross-phase modulation crosstalk in WDM networks on received power and

number of channels for various fiber types", Proc. of Asia Pacific Conference on Applied Electromagnetic (APCAE 2007), Malaysia, vol. 1, pp 22-27, 2007.

[26] Karfaa, Y. M., Ismail, M., Abbou, F. M., Shaari, S. and Majumder, S. P., "Channel spacing effects on XPM crosstalk in WDM networks for various fiber types", Proc. of IEEE 2008 6th National Conference on Telecommunication Technologies and Photonics, Malaysia, 2008.

[27] Agrawal, G. P., "Nonlinear Fiber Optic", Second Edition, Chapter 6, Academic Press, San Diego, 1995.